UNIVERSITÀ
DEGLI STUDI
DI PADOVA

Head Office: University of Padua.

Department of Cardiac, Thoracic and Vascular Sciences.

Ph.D. COURSE IN: Specialistic Medicine G.B. Morgagni

CURRICULUM: Cardiothoracic and Vascular Sciences

SERIES: XXX

MicroRNA profiling in Arrhythmogenic Cardiomyopathy and prognostic markers.

Coordinator: Prof. Annalisa Angelini.

Supervisor: Prof. Cristina Basso.

Co-Supervisor: Prof. Kalliopi Pilichou.

Ph.D. student: Maria Bueno Marinas

TABLE OF CONTENT

ABSTRACT

Background: Arrhythmogenic cardiomyopathy (AC) is a clinically and genetically heterogeneous myocardial disease, characterised by a progressive myocardial dystrophy with fibro-fatty replacement, and represents one of the major causes of sudden cardiac death in the young and athletes. Although half of AC patients harbour private desmosomal gene mutations, their low and age-dependent penetrance suggests the involvement of other regulatory molecules. MicroRNAs (miRNAs) are a group of endogenous short noncoding RNAs that regulate gene expression by sequence-specific recognition of their target transcripts. They have been associated with numerous pathophysiological conditions, including cardiovascular diseases; however, their role as key regulatory molecules in AC as well as their impact on the onset and progression of the disease is largely unknown.

Purpose: miRNA profiling in genotype-positive AC-patients with different gene mutations in order to identify their potential as AC biomarkers.

Methods: The study involved 59 subjects with a definite AC diagnosis, previously genotyped, and 14 healthy controls. 84-miRNA array was applied on 8 frozen right-ventricle (RV) myocardial tissue samples, from heart transplanted AC patients; 9 whole blood samples, from patients with definite AC diagnosis, and 6 healthy controls (HC). In the validation study, seven miRNAs were analysed on 42-AC and 8-HC blood samples. miRNA analysis was performed by qPCR, relative quantification ΔΔCt method and *in silico* target prediction. All data were expressed in fold-change values. Receiver operating characteristic (ROC) analysis was performed on validated miRNAs.

Results: miRNA profiling on AC-tissue samples displayed a genotype-related profile, 19 miRNAs were differentially expressed in PKP2 carriers, 15 in DSP carriers and 14 in DSG2 carriers, when compared to healthy controls. A common signature between PKP2 and DSP carriers was identified with 14 miRNAs in common (PKP2/DSP profile). None of these miRNAs were shown within DSG2 profile. *In silico* target prediction identified Hippo Signaling Pathway as a common target for both profiles. Analysis of AC-tissue samples as a unique group confirmed 26 differentially expressed miRNAs (AC-tissue profile) with predicted targets in the AC pathway. AC-blood miRNA profiling demonstrated a 14-miRNA signature, with 10 miRNAs differentially expressed in common with AC-tissue profile. Hsa-miR-144-3p, -122-5p, -208a-3p and -494-3p as well as hsa-miR-21-5p, -155-5p and -320a were analysed on a larger cohort of 42-AC and 8-HC. Only hsa-mir-122-5p was significantly overexpressed (p-value<0,05). ROC analysis showed hsa-miR-122-5p to be a potential AC biomarker (area under the curve: 0.83).

Conclusions: A genotype-related miRNA profile was observed in AC-tissue samples, as to reflect clinical variability. In addition, 10 miRNAs in common were identified between AC-tissue and AC-blood profiles, proving a specific miRNA signature for AC. These miRNA profiles targeted pathways involved in AC pathogenesis demonstrating their key roles in the onset and progression of the disease. Circulating level of hsa-miR-122-5p was significantly elevated in AC subjects, demonstrating its potential as a prognostic marker for heart failure in AC.

1 INTRODUCTION

1.1 Introduction of microRNA.

1.1.1 Discovery.

At the beginning of 1990s, studies in plants, nematodes and flies demonstrated an extraordinary phenomenon called *RNA interference* (RNAi). RNA interference is an evolutionary conserved genetic surveillance mechanism that can degrade mRNA in response to the presence of double-stranded RNA (dsRNA) corresponding to the targeted mRNA. Molecules of RNA neutralize mRNA by transcriptional or translational inhibition, mediated by small double-strand RNA molecules called small interference RNA (siRNA), which are the consequence of dsRNA cleavage (Ambros 2001). This occurs as an "immune system" inside cells at genetic level, in which cells protect themselves from parasitic nucleotide sequences, viruses or other foreign genetic material, in plants and animals (Hannon 2002).

When this process was fully understood, Andrew Fire and Craig C. Mello were awarded with Nobel Prize in Physiology or Medicine in 2006. They described RNAi in the nematode worm *Caenorhabditis elegans* (*C. elegans*) in 1998. In their experiments, they injected a specific dsRNA in the nematode, with the same sequence as an abundant transcript in gonad and early embryos, *mex-3*. No endogenous transcript *mex-3* was observed in animals injected with dsRNA segment during development, demonstrating a pronounced elimination of the endogenous mRNA (Fire et al., 1998)

In RNA interference process, dsRNA is bound and cleaved by a ribonuclease protein called DICER, producing small molecules of RNA called siRNA, double-stranded fragments of about 20-25 nt. These siRNA are integrated into a protein complex called RNA-interference silencing complex (RISC). One of the strands is degraded and the

other one is the “guide sequence” that interacts with a specific mRNA by base-pairing and cleaves it.

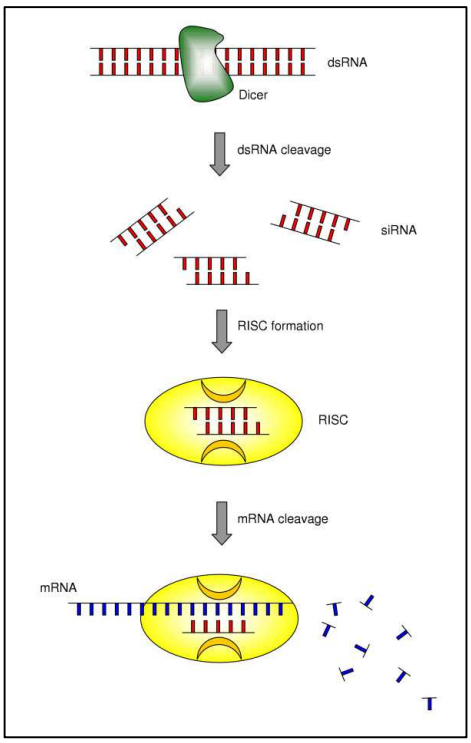

Figure 1: Schematic representation of RNA interference mechanism (from Mocellin et al. 2004).

However, it was earlier in 1993 when a first description of RNA-RNA regulation was proposed. Rosaling C. Lee and Victor Ambros studied gene *lin-4* in *C. elegans* and its role in the normal temporal control of postembryonic development. This gene acts by negatively regulating the level of protein LIN-14, creating a temporal decrease of this protein and starting the first larval stage. Their experiments demonstrated that *lin-4* does not encode for a protein but it produces two small transcripts, one of 22 nt and another of 61 nt, called small temporal RNAs (stRNA). These two transcripts contain a sequence complementary to a repeated sequence in the 3’ untranslated region (3’UTR) of *lin-14* mRNA, suggesting a RNA-RNA interaction system by which *lin-4* regulates expression of *lin-14* (Lee et al., 1993).

Subsequently, another small temporal RNA was discovered in *C. elegans* by Reinhart and colleagues in 2000. Gene *let-7* encodes for 21-nt RNA that is complementary to

elements in 3'UTR region of some genes involved in the timing of development from larva to adult, and their expression is directly controlled by *let-7* (Reinhart et al., 2000). Unlike *lin-4*, *let-7* was found to be conserved among species, from flies to humans, demonstrating that this small non-coding RNA might be important to gene regulation and development (Pasquinelli et al., 2000).

1.1.2 Definition.

Together, stRNAs and siRNAs form two types of short RNAs that serve as a guide to a direct posttranscriptional regulatory machinery to specific mRNA targets. The two small RNAs discovered in *C. elegans, lin-4* and *let-7,* are not siRNAs, they are processed from an endogenous stem-loop precursor transcript by almost the same mechanism Dicer/Risc (Ambros 2001). Nelson C. Lau and colleagues investigated the role in gene regulation of these small RNAs in *C. elegans* and reported 55 new small RNAs, with different expression patterns during development (Lau et al., 2001). Some of them were expressed temporary in a determined process and others were constitutively expressed, even some presented a tissue-specific pattern expression. They concluded that *lin-4* and *let-7* are members of a larger class of non-coding RNAs that are about 20-24 nt in length and are processed from fold-back or hairpin structures. Together with Lagos-Quintana and colleagues, and the group of Lee and Ambros, referred to these tiny RNAs as microRNAs (miRNAs) (Ambros 2001, Lagos-Quintana et al., 2001). The abundance of these tiny RNAs, their expression patterns and their evolutionary conservation imply that miRNAs might have broad regulatory functions in animals (Lau et al., 2001).

To date, more than 2500 mature miRNAs have been discovered in human (http://www.mirbase.org/; Kozomara and Griffiths-Jones 2014). We now know that miRNAs are a group of endogenous small molecules, noncoding RNA of about 17-25 nt, which regulate gene expression by degradation of mRNA or translational

repression, blocking protein synthesis (Bartel 2004). Approximately, 60% of protein-coding genes are regulated by miRNAs, conferring the potentiality of being involved in many cellular processes, normal or pathological. Some of them act as key regulators of a particular process affecting the expression of hundreds of genes simultaneously. On the other hand, others may regulate a specific mRNA target or regulate a mRNA cooperatively (Roma-Rodrigues et al., 2015)

1.1.3 miRNA biogenesis and function.

miRNA are short, endogenous, single-stranded RNA molecules that regulate gene expression. They can be expressed by an individual gene or co-expressed in clusters from different parts of genome; meaning that more than one miRNA is transcribed together by the same transcription factor. They can be excised from introns of coding-protein genes, from introns or exons of non-coding genes or even from 3' UTR of protein coding genes (Rodriguez et al., 2004)

1.1.3.1 Biogenesis.

miRNA genes are transcribed by both RNA polymerase II or RNA polymerase III into primary transcripts called pri-miRNA, hundred-nucleotides length, into the nucleus. Both polymerases are regulated differently recognising a wide diversity of promoters, permitting wide variety of regulatory options (Winter et al., 2009). This primary precursor contains a hairpin stem of 33 base-pairing nucleotides, a terminal loop and two single-stranded flanking regions upstream and downstream of the hairpin (Han et al., 2006).

A multiprotein complex (microprocessor complex) containing an endonuclease enzyme called Drosha associated with a nuclear protein named DGCR8 cleaves the 5' and 3' arms of the pri-miRNA and stabilizes the molecule, giving rise to a stem-loop secondary precursor of 70 nt named pre-miRNA (Lee et al., 2003). Both arms and the

secondary structure of pri-miRNA are critical for Drosha to recognize the substrate among all RNA molecules inside the nucleus (Han et al., 2006).

After nucleus processing, pre-miRNA is exported into the cytoplasm by Exportin-5 in complex with Ran-GTP, which transports it into the cytoplasm and protects it from exonucleolytic digestion (Yi et al., 2003). In the cytoplasm, a RNase III enzyme called Dicer recognizes the double-stranded stem and, interacting with 5' and 3' ends of the hairpin, cleaves the pre-miRNA into double-stranded miRNA, which each strand is originated from the opposite arms of the hairpin. Even though both strands of the duplex have the potentiality to interact with mRNA, the most stabilized strand (guide strand) is incorporated into the RNA-induced silencing complex (RISC), becoming mature and functional miRNA, and the other one is degraded (passenger strand). Nevertheless, sometimes both strands exhibit similar stability and each strand is integrated into the complex with similar frequency (Schwarz et al., 2003).

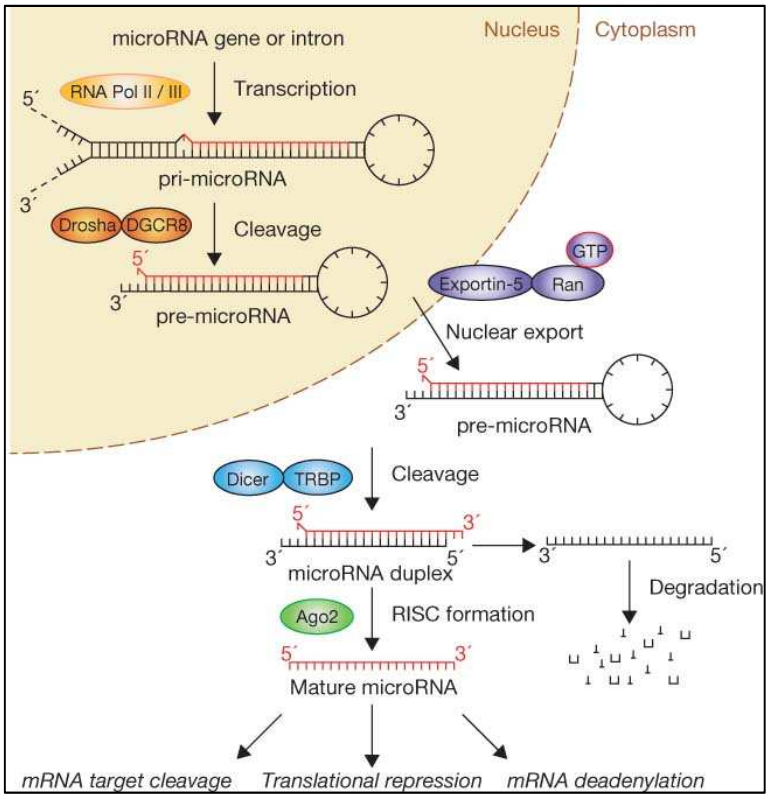

Figure 2: Biogenesis of mature miRNA (from Winter J. et al, 2009).

1.1.3.2 Function.

The RISC complex associated with mature miRNA is also called microRNA ribonucleoprotein complex (miRNP). A key protein inside the complex is Argonaute protein (AGO) that presents two domains by which it binds the mature miRNA and orients it for interaction with a target mRNA. It's the "RISC effector" mediating mRNA degradation or translational inhibition (Meister et al., 2004). The choice between mRNA degradation or translation inhibition mechanisms depends on miRNA sequence complementary with its target. When miRNA sequence perfectly matches with its target, AGO cleaves the mRNA and leads to direct degradation. Instead, when AGO-miRNA lacks complementary, mRNA translation is inhibited blocking protein synthesis (Doench et al., 2003). In animals, vast majority of AGO proteins do not induce target cleavage but translation repression by three different mechanisms: blocking translational initiation, blocking elongation or leading to deadenylation (Ameres and Zamore 2013).

miRNAs regulate gene expression by base pairing at sites in 3' UTR of target mRNA. Bound specificity is only represented by 6 to 7 nucleotides from the above 20 of the mature miRNA, located between 2 to 8 nucleotides of 5' end, calling this region as "seed region" (Lai 2002). Computationally prediction of miRNA-mRNA complementarity showed that one miRNA has the potentiality of inhibiting more than 200 mRNAs. But also, binding just a single miRNA might not be enough to block translation and several miRNAs are necessary to regulate a single mRNA (Bartel 2004).

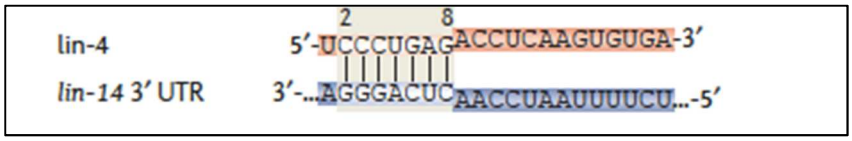

Figure 3: Schematic representation of interaction between miRNA *lin-4* and its target *lin-14* in *C. elegans*: 2 to 8 nucleotides in 5' end of miRNA bind 3' UTR of mRNA (from Ameres and Zamore, 2013).

1.1.4 Location in genome.

The total length of the human genome is over 3 billion base pairs, and only 2% is coding DNA, meaning that only 2% are transcribed into mRNA and translated into proteins. The other 98%, non-coding DNA, comprise genes coding for RNA molecules with important functions inside cells, non-coding RNAs (miRNA, small nucleolar RNAs), which their regulatory functions are essential to biological processes, or ribosomal or transfer RNAs, which are involved in protein translation.

The location and structure of miRNA genes are not perfectly defined, but above 40% of miRNAs are found and expressed in clusters, for example cluster miR-17-92 encodes for a polycistronic precursor that gives rise to 7 mature miRNAs (hsa-miR-17-3p/5p, hsa-miR-18a, hsa-miR-19a, hsa-miR-19b, hsa-miR-20a and hsa-miR-92a) (Griffiths-Jones et al., 2008). They frequently contain representatives from different miRNA families, meaning that miRNAs of the same cluster can target multiple different mRNAs (Yuan et al., 2009). It is also possible to find a single miRNA in intergenic regions with its own promoter. Moreover, a number of miRNA genes have been discovered in other transcription units of other genes, intronic and exonic regions (Lagos-Quintana et al., 2001), in both sense and anti-sense chains, and their expression is correlated with the host gene expression. They can be expressed by their own promoters or excised from introns or exons during splicing (Olena and Patton 2010).

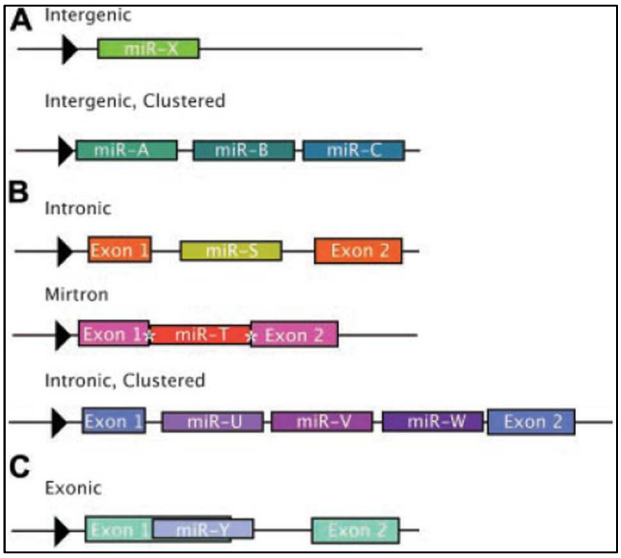

Figure 4: Schematic representation of miRNA genes location in genome (from Olena and Patton, 2014).

1.1.5 Nomenclature.

miRNAs are named based on a standard nomenclature system. To now, they are known 2588 human mature miRNAs (miRBase, release 21). The prefix “miR-“ indicates mature miRNA, instead “mir-“ is used for pre-miRNA while “MIR-“ refers to the gene that encodes them. A number goes after the dash and is assigned based on new experimentally confirmed miRNA, lower number indicates earlier discovery. When two miRNAs have nearly identical sequences with 1 or 2 different nucleotides, they are annotated with an additional letter (for example. miR-29a or miR-29c). Instead, when they are from the two different arms of the hairpin, they are denoted with -3p (from 3’ arm) or –5p (from 5’ arm) suffix (for example, miR-21-3p and miR-21-5p). Finally, three letters are added at the beginning to indicate the specie of origin, when “hsa” is used for human (hsa-miR-21-5p) (Ambros et al., 2003).

1.1.6 Stability.

Little is known about half-life and degradation of mature miRNA, but they are quite stable in cells and it has been demonstrated that they also have a role in cell-to-cell communication (Creemers et al., 2012, Winter et al., 2009). They can be packed in microvesicles, exosomes or apoptotic bodies in circulation, allowing resistance even to high/low temperature, pH changes and multiple freeze/thaw cycles. They are present in all blood compartments, including plasma, platelets, erythrocytes and nucleated blood cells (Latronico and Condorelli 2009). They bind RNA-binding proteins or linkage high-density lipoproteins, forming miRNA-protein complexes, conferring them protection from circulating RNases (Creemers et al., 2012). Circulating miRNAs can be released from apoptotic or necrotic cells during cell death process; either free miRNAs aggregate to RNA-binding proteins or limited into apoptotic bodies. Circulating miRNAs may also be released by active secretion cells acting as signals for cell-to-cell communication within exosomes or vesicles (Schwarzenbach et al., 2014).

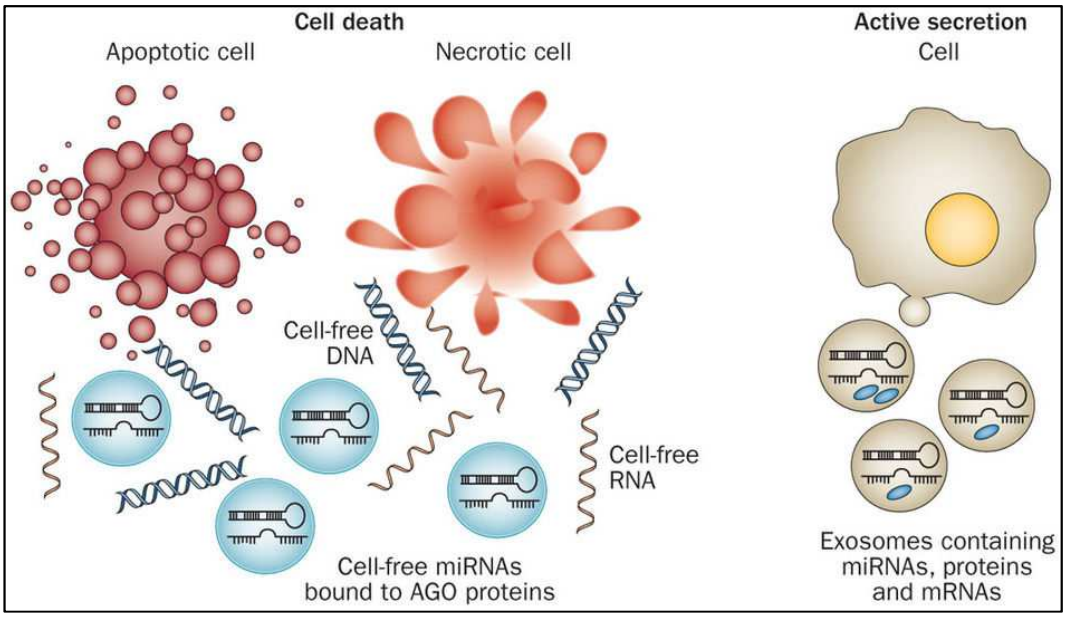

Figure 5: Schematic representation of miRNA release from cell death or active secretion cells (from Schwarzenbach et al., 2014).

1.1.7 Role of miRNA in normal development and differentiation.

Since miRNA discovery in *C. elegans*, we now know that miRNAs play an important role in every biological process. Both *lin-4* and *let-7* are correlated with *C. elegans* development and they are expressed in a determined phase of development and during a specific time, demonstrating a specific pattern and timing of expression (Bartel 2004). After numerous studies, miRNA involvement in differentiation, proliferation, apoptosis or metabolism is indisputable, and understanding their specific regulatory functions in cells and their expression profiles has been the focus of recent research.

For example, numerous studies demonstrated the importance of cluster hsa-miR-17-92 in cardiac development, both in embryonic and postnatal hearts, and its involvement in normal proliferation of cardiac blood vessels cells (Fiedler and Thum 2016). Two other miRNAs involved in heart development are hsa-miR-1 and hsa-miR-133 families. Hsa-miR-1 is first detected during the beginning of muscle differentiation and then become progressively more expressed, first only in inner curvature of heart loop and in atria, but then ubiquitously expressed as development continues (Latronico and Condorelli 2015). On the other hand, hsa-miR-133 is expressed in the heart and the skeletal muscle, increasing their expression during development as observed in mice. It inhibits differentiation and promotes proliferation of myoblasts (Latronico and Condorelli 2015). Timing and tissue-specific expression is observed in heart development, thus aberrant expression of miRNA can lead to dysregulated development and, as a consequence, to pathological conditions.

1.1.8 Role of miRNA in human diseases.

As miRNAs are involved in normal functioning of cells, their regulation also plays a role in pathological conditions and it has been demonstrated an aberrant expression profile of miRNA during diseases. The first human condition associated with miRNA deregulation was Chronic Lymphocytic Leukemia (Calin et al., 2002), and since then,

differences in miRNA expression have been identified as characteristic in pathological conditions. Not only miRNA expression is important but also mutations in seed regions or deletion of some miRNA have been involved in diseases, for example a mutation in the seed region of hsa-miR-96 causes hereditary progressive hearing loss (Mencía et al., 2009).

Indeed, numerous studies have identified specific expression profiles of miRNA in different type of cancers. Over or under-expression of determined miRNAs plays a crucial role in tumour initiation, progression and metastasis. For example, overexpression of hsa-miR-21 or cluster hsa-miR-17-92 works as an “oncogene” by targeting tumour suppressor genes as PTEN and E2F1 in solid and hematologic malignancies, respectively. These miRNAs are also called oncomirs. Instead, underexpression of miRNAs, as let-7 in lung cancer (Landi et al., 2010) or hsa-miR-15/16 in leukemia, operates as tumour suppressor genes by under-regulating Ras and BCL2, respectively. Researchers continue to study miRNA expression profile in order to understand their mechanism in cancer and to use them as biomarkers or even targets for therapy (Yu et al., 2011).

Further, miRNAs also play an important role in cardiovascular diseases and several plasma miRNAs have been identified as specific for cardiovascular pathologies, for example in Acute Myocardial Infarction (AMI) (Creemers et al., 2012). It is thought that during myocardial infarction, heart-specific miRNAs leak into the circulation and four have been identified with elevated levels in plasma of AMI patients: hsa-miR-208a, hsa-miR-499, hsa-miR-1 and hsa-miR-133 (Corsten et al., 2010, Kuwabara et al., 2011). miRNA profile expression was also studied in Coronary Artery Disease (CAD) and it has been reported that levels of three endothelial-enriched miRNAs (hsa-miR-126, hsa-miR-92a and hsa-miR-17), levels of hsa-miR-145 (enriched in smooth-muscle cells) and levels of hsa-miR-155 (associated with inflammation) were significantly reduced in CAD patients compared to controls (Fichtlscherer et al., 2010).

The expression profile of miRNAs has been studied and it has been demonstrated a dysregulation of miRNA levels in pathological conditions compared to healthy subjects. Besides, their stability and presence in circulating biofluids in addition to their non-invasive detection methods and their disease-specificity turn them into promising biomarkers and even potential therapeutic targets (Creemers et al., 2012).

1.2 Cardiomyopathies.

1.2.1 Definition.

The current definition of cardiomyopathy is: a heterogeneous group of diseases of the myocardium associated with mechanical and/or electrical dysfunction that usually exhibit inappropriate ventricular hypertrophy or dilatation and are due to a variety of causes that frequently are genetic. Cardiomyopathies are confined to the heart or are part of generalized systemic disorders, often leading to cardiovascular death or progressive heart failure-related disability (Maron et al., 2006). They are usually associated with failure of myocardial performance, which can be mechanical or electrical (such as ion channelopathies).

1.2.2 Classification.

Cardiomyopathies are divided into two major groups, depending on the predominant organ involved.

- Primary cardiomyopathies: solely or predominantly confined to heart muscle and relatively few in number. They can be genetic, nongenetic or acquired. Among genetic forms of primary cardiomyopathies, we can find Arrhythmogenic Cardiomyopathy, Hypertrophic Cardiomyopathy (HCM) and Dilated Cardiomyopathy (DCM).

- Secondary cardiomyopathies: show pathological myocardial involvement as a part of a large number of generalized systemic disorders, i.e. aortic dissection in Marfan syndrome (Maron et al., 2006).

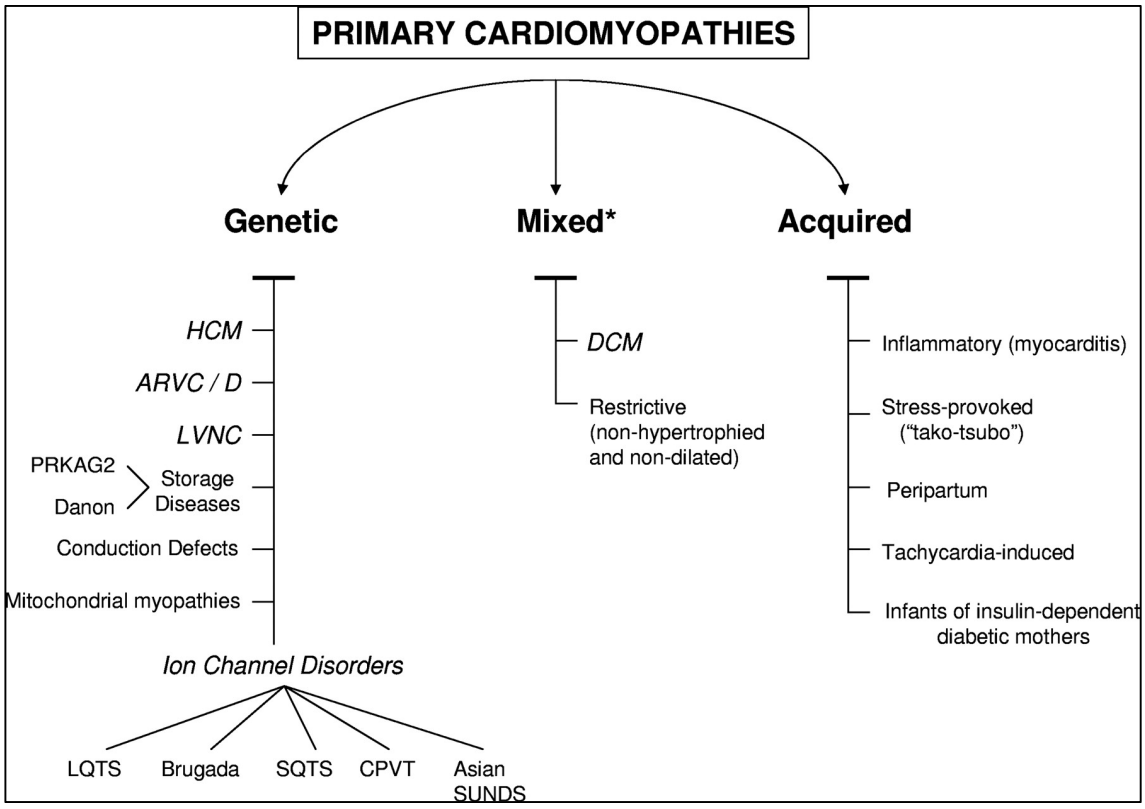

Figure 6: Primary cardiomyopathy classification (from Maron et al., 2006).

1.3 Arrhythmogenic Cardiomyopathy.

1.3.1 Definition.

Arrhythmogenic cardiomyopathy (AC) is a rare disease, with an estimated prevalence in general population from 1:2000 to 1:5000, characterized by a progressive myocardial dystrophy with fibro-fatty replacement. This process is associated with structural and functional changes involving predominantly the right ventricle (RV). Structural manifestations mainly include ventricular dilatation, hypokinesia and aneurysms of the ventricle wall. It is a "primary" cardiomyopathy genetically determined

caused by heterozygous or compound heterozygous mutations in genes mostly encoding proteins of the demosomal complex, found in about 50% of probands (Basso et al., 2009, Thiene 2015). AC shows an age-related and incomplete penetrance, presenting palpitations, syncope or cardiac arrest usually in adolescence or young adulthood, and represents one of the major causes of sudden cardiac death in the young and athlete (Thiene et al., 1988).

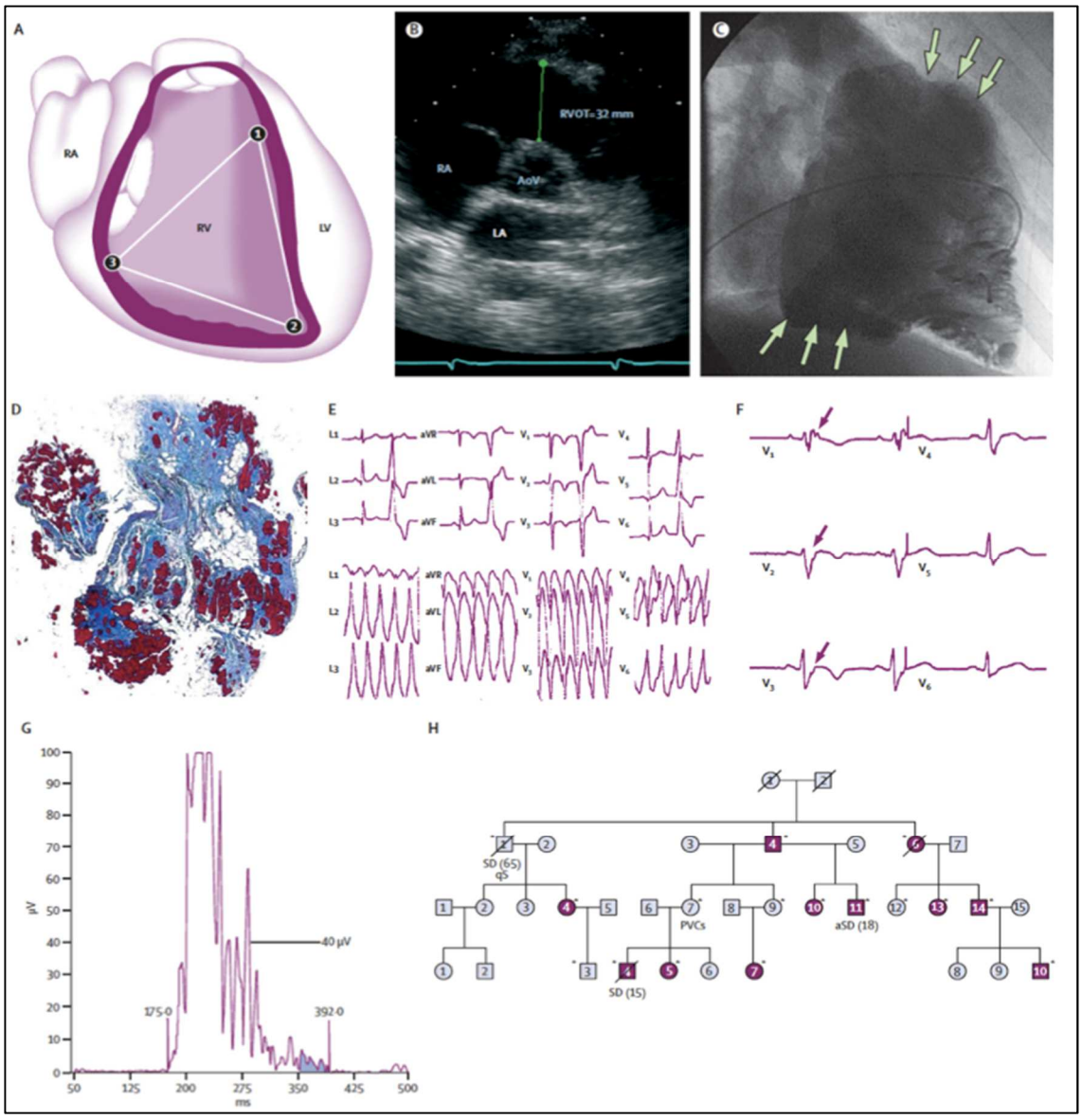

Figure 7: Diagnostic morphofunctional, electrocardiographic and tissue characteristic features of AC. (A) Triangle of dysplasia, which shows the characteristic areas for structural and functional abnormalities of RV. (B) 2-D echocardiography showing RV outflow tract enlargement. (C) RV contrast angiography. (D) Endomyocardial biopsy sample with extensive myocardial atrophy and fibro-fatty replacement. (E) 2-lead ECG with inverted T waves. (F) ECG showing post-excitation epsilon wave. (G) Signal-averaged ECG with late potentials. (H) Family pedigree (Basso et al., 2009).

1.3.2 Clinical characteristics.

Clinical diagnosis of AC is complicated as it is necessary more than one diagnostic test to ascertain the disease. Diagnosis is based on classification of clinical findings according to specific international criteria defined by an International Task Force in 1994 (McKenna et al., 1994), with additional modifications in 2010 (Marcus et al., 2010). Structural, histological, electrocardiographic, arrhythmic and familial features of the disease are described, subdivided into major and minor categories according to the specificity of their association with AC. The definitive diagnosis requires the fulfilment of 2 major, 1 major plus 2 minor, or 4 minor criteria.

AC presents a high clinical variability resulting in the absence of a single gold standard for the diagnosis. Diagnosis is based on functional and structural alterations of the RV, fibro-fatty replacement of the myocardium, depolarization and repolarization abnormalities, arrhythmias with the left bundle branch block morphology and family history (Marcus et al., 2010).

Clinical manifestations vary greatly based on age and stage of the disease. Premature ventricular complexes or ventricular tachycardia with left bundle branch block (LBBB) morphology and T-wave inversion in V1-V3 leads on basal electrocardiogram is the most common index of suspicion. Less-common presentations include right-ventricular or biventricular dilatation, with or without failure symptoms, similar to dilated cardiomyopathy characteristics (Pilichou et al., 2016).

There are four phases in a “classic” AC:

1. “Concealed”, with nearly undetectable right-ventricular structural changes, with or without arrhythmias.
2. “Overt electrical disorder”, with symptomatic ventricular arrhythmias which are life-threatening associated with clearly morpho-functional abnormalities in the RV.

3. “Right-ventricular dysfunction”, due to progression and extension of right-ventricular damage.
4. “Biventricular failure”, caused by pronounced fibro-fatty replacement in both ventricles.

Unfortunately, electrical instability may lead to arrhythmic sudden death any time during the course of the disease.

Original task force criteria	Revised task force criteria
I. Global or regional dysfunction and structural alterations*	
Major	
	By 2D echo:
• Severe dilatation and reduction of RV ejection fraction with no (or only mild) LV impairment • Localized RV aneurysms (akinetic or dyskinetic areas with diastolic bulging) • Severe segmental dilatation of the RV	• Regional RV akinesia, dyskinesia, or aneurysm • *and* 1 of the following (end diastole): — PLAX RVOT ≥32 mm (corrected for body size [PLAX/BSA] ≥19 mm/m^2) — PSAX RVOT ≥36 mm (corrected for body size [PSAX/BSA] ≥21 mm/m^2) — *or* fractional area change ≤33%
	By MRI:
	• Regional RV akinesia or dyskinesia or dyssynchronous RV contraction • *and* 1 of the following: — Ratio of RV end-diastolic volume to BSA ≥110 mL/m^2 (male) or ≥100 mL/m^2 (female) — *or* RV ejection fraction ≤40%
	By RV angiography:
	• Regional RV akinesia, dyskinesia, or aneurysm
Minor	
	By 2D echo:
• Mild global RV dilatation and/or ejection fraction reduction with normal LV • Mild segmental dilatation of the RV • Regional RV hypokinesia	• Regional RV akinesia or dyskinesia • *and* 1 of the following (end diastole): — PLAX RVOT ≥29 to <32 mm (corrected for body size [PLAX/BSA] ≥16 to <19 mm/m^2) — PSAX RVOT ≥32 to <36 mm (corrected for body size [PSAX/BSA] ≥18 to <21 mm/m^2) — *or* fractional area change >33% to ≤40%
	By MRI:
	• Regional RV akinesia or dyskinesia or dyssynchronous RV contraction • *and* 1 of the following: — Ratio of RV end-diastolic volume to BSA ≥100 to <110 mL/m^2 (male) or ≥90 to <100 mL/m^2 (female)
II. Tissue characterization of wall	
Major	
• Fibrofatty replacement of myocardium on endomyocardial biopsy	• Residual myocytes <60% by morphometric analysis (or <50% if estimated), with fibrous replacement of the RV free wall myocardium in ≥1 sample, with or without fatty replacement of tissue on endomyocardial biopsy
Minor	• Residual myocytes 60% to 75% by morphometric analysis (or 50% to 65% if estimated), with fibrous replacement of the RV free wall myocardium in ≥1 sample, with or without fatty replacement of tissue on endomyocardial biopsy
III. Repolarization abnormalities	
Major	• Inverted T waves in right precordial leads (V_1, V_2, and V_3) or beyond in individuals >14 years of age (in the absence of complete right bundle-branch block QRS ≥120 ms)
Minor	
• Inverted T waves in right precordial leads (V_2 and V_3) (people age >12 years, in absence of right bundle-branch block)	• Inverted T waves in leads V_1 and V_2 in individuals >14 years of age (in the absence of complete right bundle-branch block) or in V_4, V_5, or V_6 • Inverted T waves in leads V_1, V_2, V_3, and V_4 in individuals >14 years of age in the presence of complete right bundle-branch block

(Continued)

Original task force criteria	Revised task force criteria
IV. Depolarization/conduction abnormalities	
Major	
• Epsilon waves or localized prolongation (>110 ms) of the QRS complex in right precordial leads (V_1 to V_3)	• Epsilon wave (reproducible low-amplitude signals between end of QRS complex to onset of the T wave) in the right precordial leads (V_1 to V_3)
Minor	
• Late potentials (SAECG)	• Late potentials by SAECG in ≥1 of 3 parameters in the absence of a QRS duration of ≥110 ms on the standard ECG • Filtered QRS duration (fQRS) ≥114 ms • Duration of terminal QRS <40 μV (low-amplitude signal duration) ≥38 ms • Root-mean-square voltage of terminal 40 ms ≤20 μV • Terminal activation duration of QRS ≥55 ms measured from the nadir of the S wave to the end of the QRS, including R′, in V_1, V_2, or V_3, in the absence of complete right bundle-branch block
V. Arrhythmias	
Major	
	• Nonsustained or sustained ventricular tachycardia of left bundle-branch morphology with superior axis (negative or indeterminate QRS in leads II, III, and aVF and positive in lead aVL)
Minor	
• Left bundle-branch block-type ventricular tachycardia (sustained and nonsustained) (ECG, Holter, exercise) • Frequent ventricular extrasystoles (>1000 per 24 hours) (Holter)	• Nonsustained or sustained ventricular tachycardia of RV outflow configuration, left bundle-branch block morphology with inferior axis (positive QRS in leads II, III, and aVF and negative in lead aVL) or of unknown axis • > 500 ventricular extrasystoles per 24 hours (Holter)
VI. Family history	
Major	
• Familial disease confirmed at necropsy or surgery	• ARVC/D confirmed in a first-degree relative who meets current Task Force criteria • ARVC/D confirmed pathologically at autopsy or surgery in a first-degree relative • Identification of a pathogenic mutation[‡] categorized as associated or probably associated with ARVC/D in the patient under evaluation
Minor	
• Family history of premature sudden death (<35 years of age) due to suspected ARVC/D • Familial history (clinical diagnosis based on present criteria)	• History of ARVC/D in a first-degree relative in whom it is not possible or practical to determine whether the family member meets current Task Force criteria • Premature sudden death (<35 years of age) due to suspected ARVC/D in a first-degree relative • ARVC/D confirmed pathologically or by current Task Force Criteria in second-degree relative

Figure 8: Comparison of original and revised Task Force Criteria for diagnosis of AC (from Marcus et al. 2010).

A comprehensive workup involves the study of full family history, with particular focus on cardiac symptoms, unexplained heart failure (HF) or occurrence of sudden death. The value of AC genetic testing has been widely recognized and detection of a pathogenic variant now contributes as a major diagnostic criterion for the diagnosis of AC (Basso et al., 2009, Thiene et al., 2007).

1.3.3 Genetic features and desmosomes.

AC is considered a disorder of the desmosomes due to the identification of causative variants in different component of cardiac desmosomes that have been found in approximately 50% of AC subjects (Basso et al., 2012b).

Desmosomes are molecular complexes of cell adhesion proteins localized randomly around cell membranes permitting cell-to-cell adhesion and even intercellular communication. They are particularly abundant in epithelium and myocardium, tissues with mechanical stress. In cardiomyocytes, desmosomes connect cytoskeleton to cell membranes of adjacent cells permitting anchorage between cells, and also play a role in cell-cell communication, tissue differentiation and apoptosis (Garrod and Pickering 2009).

Desmosomes form electron-dense symmetrical structures, with a dense membrane-associated plaques intercalated by 30 nm of intercellular space, which is divided by a central midline creating the extracellular core domain and the intracellular plaque. Two areas form the intracellular plaque: the outer dense plaque and the inner dense plaque (North et al., 1999). In the outer plaque, cytoplasmatic domains of desmoglein 2 (DSG2) and desmocollin 2 (DSC2) (belonging to cadherin family) bind desmoplakin (DSP) (from plakin family) through plakophilin 2 (PKP2) and plakoglobin (JUP), which are armadillo proteins. Instead, in the inner plaque, plakins attach intermediate filaments of the cell, providing cellular adhesion and structural integrity.

The comprehension that AC is a cell-adhesion disorder was first observed in Naxos syndromic patients. This syndrome is characterized by abnormalities on the heart (AC), skin (palmoplantar keratosis) and hair (woolly hair), tissues with similar junction structures. It is an autosomal recessive syndrome and mutations in the gene encoding JUP, which is a major constituent of desmosomal complex, were the first disease-causing mutations identified in an AC recessive form (McKoy et al., 2000). Furthermore, mutations in the gene encoding another desmosomal component (DSP)

were identified in another cardiocutaneous syndrome called Carvajal syndrome, also related with junction abnormalities (Norgett et al., 2000).

Up to date, mutations in 5 desmosomal-coding genes have been identified, which encode major molecular components of desmosomes: DSC2, DSG2, DSP, JUP and PKP2 (Gerull et al., 2004, McKoy et al., 2000, Norgett et al., 2000, Pilichou et al., 2006, Syrris et al., 2006). Mutations may be transmitted either as recessive or dominant traits (Corrado et al., 2017). Furthermore, mutations in non-desmosomal proteins were also associated with AC, such as RYR2 (ryanodine receptor 2), TGFB3 (transforming growth factor beta3), TMEM43 (transmembrane protein 43), DES (desmin) or TTN (titin) (Corrado et al., 2017).

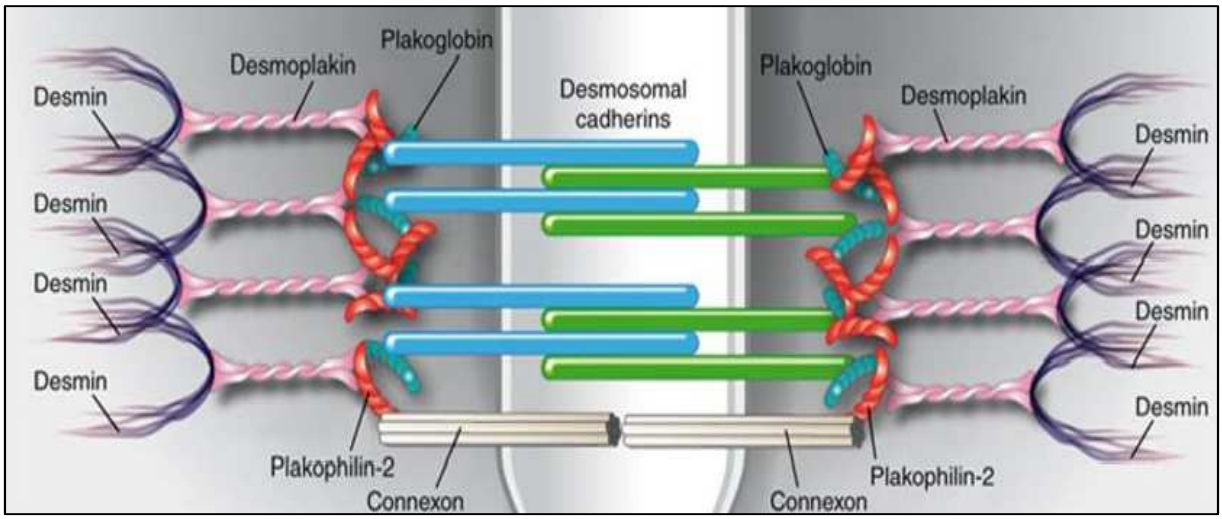

Figure 9: Schematic representation of desmosome components (from Pilichou et al., 2017).

1.3.4 Pathogenesis.

Various pathophysiological mechanisms have been proposed in order to explain AC pathogenesis. In 1996, the myocardial dystrophy (degenerative theory) was postulated before discovering disease-causing gene mutations, however it remains the most comprehensive theory. There is a similarity between AC and skeletal-muscle dystrophies, consisting in acquired and progressive muscular atrophy with fibro-fatty

tissue replacement. In AC there is a progressive loss of ventricular myocardium as a consequence of progressive loss of cardiomyocytes by apoptosis or necrosis leading to fibro-fatty replacement (Pilichou et al., 2009). The role of desmosomes remains unclear, but as they are crucial for cell-to-cell adhesions and intermediate filament strength, it is thought that cytoskeletal impairment or abnormal intracellular homeostasis may lead to cardiomyocyte death.

Inflammatory theory proposed AC as a consequence of a preceding myocarditis, since myocardial inflammation is a common feature in hearts with AC (Thiene et al., 1991). Other studies considered that viral myocarditis overlay on an already affected heart, accelerating the progression of the disease instead of being involved as a primary factor (Calabrese et al., 2006).

In the transdifferentiation theory, cardiac myocytes are thought to undergo a metamorphosis, switching to adipocytes (d'Amati et al., 2000). This theory is supported by the idea that adipocytes in AC derive from progenitor cells of the second heart field. The progenitor cells switch into adipocytes because of the suppression of Wnt/β-catenin signaling pathway as a result of JUP translocation to the nucleus (Garcia-Gras et al., 2006). This pathway is known to regulate adipogenesis, fibrogenesis and apoptosis.

Most recently, desmosomes disruption was also linked to the activation of Hippo/Yes-associated protein (YAP) pathway. Activation or inhibition of this pathway regulates cardiomyocyte proliferation and as a consequence, heart size and shape (Chen et al., 2014), suggesting a connection between molecular changes in intercalated disc (ID) and Wnt/β-catenin and Hippo/YAP pathway. The trigger for Hippo signaling pathway activation is presumed to be the impairment assembly of IDs, activating neurofibromin (NF2 or Merlin) and as a consequence, a cascade of phosphorylation events including mammalian STE20-like protein kinases 1/2 (MST1/2), large tumor suppressor kinases 1/2 (LATS1/2) and yes associated protein (YAP). The latter is the effector of the Hippo

pathway, and is inactivated when phosphorylated. Consequently, gene expression through YAP-TEAD is suppressed. As Hippo signaling pathway regulates myocyte proliferation it has been postulated that YAP inactivation may be associated with myocyte atrophy. In addition, YAP binds to β-catenin and JUP, sequestering β-catenin and inactivating the canonical Wnt/β-catenin pathway too, enhancing adipogenesis (Chen et al., 2014).

Unfortunately, the role of desmosomal gene mutations in the pathophysiology of myocardial injury remains elusive (Basso et al., 2012a). Desmosome composition, function and junction organization may be influenced by mutations in genes coding for the major components of desmosomes (*DSP, DSG2, DSC2, PKP2, JUP*), and as a consequence, alteration in the correlated pathways (Wnt/β-catenin, Hippo/YAP). Pathogenic variants in desmosomal genes may lead to abnormal proteins that might result into an incorrect assembly or non-functional desmosomes, or into insufficient incorporation of a normal protein, or into the loss of essential protein-protein interactions. Therefore, they cause a disruption of desmosomes structures resulting in the reduction of mechanical contact between cells, so myocytes can lose adhesion causing cell death (Delmar and McKenna 2010). As the cardiac myocytes have a limited regenerative capacity, cell death may activate a repair mechanism implying replacement by fibrous and adipose tissue.

Another possible effect of abnormal demosomal components may result in a re-organization of structural cardiac junctions, known as area composita (Franke et al., 2006). The remodelling of gap junction assembly may lead to an impairment of connexin 43 localization, resulting in heterogeneous conduction of the electric impulse and explaining the propensity of arrhythmias in AC patients (Asimaki and Saffitz 2014, Kleber and Saffitz 2014, Patel et al., 2014).

Desmosomal components are also involved in intercellular signaling, and for example, translocalization of JUP may supress the canonical Wnt/β-catenin signaling pathway,

increasing expression of transcriptional regulators of adipogenesis and causing the switch from second field cardiac stem cells into adipocytes (Garcia-Gras et al., 2006, Lombardi et al., 2011).

2 AIM OF THE STUDY

The relevance of miRNAs in pathophysiology of cardiovascular diseases is increasing showing their potential as diagnostic and prognostic biomarkers and therapy targets. A characteristic miRNA expression profile has been demonstrated in the most significant primary cardiomyopathies (HCM, DCM and AC). However, there is no consistency in results among studies. Specifically, in AC very few studies have been carried out to demonstrate the implication of miRNAs in disease pathogenesis. Thus, further studies are needed in order to determine miRNA expression profile and their role in AC as disease modifiers. The aim of the study is the identification of a specific miRNA expression profile both in circulation and tissue specific of AC in order to determine their potential as diagnostic and prognostic biomarkers.

3 MATERIAL AND METHODS

3.1 Study cohort.

The study involved 59 subjects with a clinical diagnosis of AC referred to Referential Clinical Genetic Centre of Arrhythmic Cardiomyopathies in Padua. In addition, 12 healthy subjects and 2 subjects non-affected by cardiovascular diseases were used as controls.

It has been analysed frozen myocardial tissue samples from RV of transplanted hearts from 8 of 59 subjects and frozen whole blood samples from the rest 51 subjects (AC group). As controls, 2 RV myocardial tissue samples were analysed from autopsy of subjects non-affected by cardiovascular diseases and 12 blood samples of healthy subjects (HC).

AC subjects previously underwent genetic screening by Next Generation Sequencing or Sanger Sequencing technologies and were classified based on desmosomal mutated genes as represented in table 1.

Subject	Type of sample	Desmosmal mutation	Subject	Type of sample	Desmosmal mutation
1	RV myocardial tissue	PKP2	31	Whole blood	DSG2 + DSG2
2	RV myocardial tissue	PKP2	32	Whole blood	PKP2
3	RV myocardial tissue	PKP2	33	Whole blood	PKP2
4	RV myocardial tissue	DSP	34	Whole blood	DSG2
5	RV myocardial tissue	DSP	35	Whole blood	DSP + PKP2
6	RV myocardial tissue	DSP	36	Whole blood	DSC2
7	RV myocardial tissue	DSG2	37	Whole blood	PKP2
8	RV myocardial tissue	DSG2	38	Whole blood	DSG2 + PKP2
9	Whole blood	PKP2	39	Whole blood	DSG2 + PKP2
10	Whole blood	PKP2	40	Whole blood	DSP
11	Whole blood	PKP2	41	Whole blood	PKP2
12	Whole blood	PKP2	42	Whole blood	DSP
13	Whole blood	PKP2	43	Whole blood	DSC2
14	Whole blood	DSG2	44	Whole blood	DSC2
15	Whole blood	DSP	45	Whole blood	DSG2
16	Whole blood	DSG2 + DSC2	46	Whole blood	Gen NEG
17	Whole blood	DSG2 + DSP	47	Whole blood	DSP
18	Whole blood	DSP	48	Whole blood	PKP2
19	Whole blood	Gen NEG	49	Whole blood	DSP
20	Whole blood	PKP2	50	Whole blood	PKP2
21	Whole blood	PKP2	51	Whole blood	PKP2 + PKP2
22	Whole blood	PKP2	52	Whole blood	PKP2
23	Whole blood	PKP2	53	Whole blood	PKP2
24	Whole blood	DSC2	54	Whole blood	PKP2
25	Whole blood	DSG2 + PKP2	55	Whole blood	PKP2
26	Whole blood	DSG2	56	Whole blood	PKP2
27	Whole blood	DSC2	57	Whole blood	DSP
28	Whole blood	PKP2 + DSC2	58	Whole blood	DSC2
29	Whole blood	DSG2	59	Whole blood	PKP2
30	Whole blood	PKP2			

Table 1: Desmosomal mutations and type of samples from the 59 AC subjects.

3.2 miRNA isolation from frozen myocardial tissue.

Different methods have been tested to isolate miRNAs from frozen myocardial tissue samples in order to determine which one resulted in higher quality, quantity and less inhibitors. A total of 4 protocols with two different commercial kits were performed: miRNeasy Mini Kit (Qiagen, Hilden, Germany) with total RNA isolation, miRNeasy Mini Kit (Qiagen, Hilden, Germany) with enrichment of small RNAs, RNeasy Mini Kit (Qiagen, Hilden, Germany) with total RNA isolation (modified protocol) plus RNA clean-up, RNeasy Mini Kit (Qiagen, Hilden, Germany) with enrichment of small RNAs.

RNeasy Mini Kit with a modified protocol and followed by clean-up procedure of RNA was chosen to isolate RNA from myocardial tissue samples. 20 mg of frozen myocardial tissue were disrupted with TissueLyzer II (Qiagen, Hilden, Germany) adding 700 µl of Qiazol (Qiagen, Hilden, Germany), performing cycles of 30 seconds with 25.0 of frequency until the tissue was completely homogenized. The tube containing the homogenate was placed on the benchtop at room temperature (15–25°C) for 5 minutes. This step promotes dissociation of nucleoprotein complexes. Afterwards, 10 µl of Proteinase K (Roche, Mannheim, Germany) were added and the sample was incubated 10 minutes at 55°C.

After incubation, 140 µl of chloroform were added to the sample and the tube was shaken vigorously for 15 seconds and placed in the benchtop at room temperature during 3 minutes. The sample was then centrifuged for 15 minutes at 12000 x g at 4°C, in order to separate the different phases. After centrifugation, the sample is separated in three phases: an upper, colorless, aqueous phase containing RNA; a white interphase; and a lower, red, organic phase. The upper colorless phase was then transferred carefully to another reaction tube where 1.5 volumes of 100% ethanol were added in order to precipitate not only large RNA but also small RNA (including miRNA). The sample was pipetted immediately into the RNeasy Mini spin column and centrifuged at 8000 x g for 15 seconds at room temperature. The flow-through was

discarded and 350 µl of buffer RW1 were added, then the tube was centrifuged at 8000 x g for 15 seconds at room temperature. The flow-through was again discarded and 80 µl of DNase (Qiagen, Hilden, Germany) were added carefully at the top of the filter and the sample was incubated during 20 minutes at room temperature in order to degrade genomic DNA remaining in the sample.

Afterwards, 350 µl of buffer RW1 were added and the tube was centrifuged at 8000 x g for 15 seconds at room temperature. Two washes with RPE buffer were the next step in which 500 µl were added to the sample, then the tube was centrifuge and the flow-through was discarded. In the second wash, the tube was centrifuge at 8000 x g for 2 minutes. Finally, total RNA including small RNA were eluted by adding 30 µl of nuclease-free water, incubating the sample during at least 10 minutes and then centrifuging at 8000 x g for 1 minute. The flow-through was total RNA extract including small RNAs such as miRNAs.

Afterwards, 20 µl of isolated total RNA was cleaned up following RNeasy Clean up protocol with some modifications. The volume was first adjusted to 100 µl with RNase-free water and then 350 µl of buffer RLT were added. 700 µl of 100% ethanol were added into the sample and then transferred into a RNeasy Mini Spin column, which was centrifuged at 8000 x g for 15 seconds. The flow-through was discarded and two washes steps with RPE buffer were performed. Finally, total RNA was eluted in 30 µl of RNeasy-free water.

3.3 miRNA isolation from whole blood.

Blood was collected in anti-coagulant EDTA tubes and then conserved at -80°C until RNA isolation. Total RNA including small RNA was isolated from whole frozen blood samples with MagMAX *mir*Vana Total RNA Isolation Kit (ThermoFisher Scientific, Waltham, MA, USA) following user manual. Briefly, 30 µl of PK Digestion Mix were added to 50 µl of whole blood and shaken during 5 minutes at 900 rpm in Thermomixer

compact (Eppendorf, Hamburg, Germany). The mix was then incubated during 10 minutes at 65°C. Magnetic binding beads were then added to the mixture (20 µl of Binding Beads Mix, previously prepared) and the sample was shaken during 5 minutes at 800 rpm. Afterwards, Lysis Mix was prepared adding β-mercaptoethanol to the lysis buffer (1:100), and then 65 µl were added to the sample. The tube was then agitated 5 minutes at 700 rpm. 135 µl of isopropanol were added to the sample and then the tube was shaken during 10 minutes at 500 rpm.

The sample was then processed on the Magnetic Stand-96 (Ambion by ThermoFisher Scientific, Waltham, MA, USA) for 5 minutes. The supernatant was carefully aspirated and discarded (RNA is bound to the beads). The tube was removed from the Magnetic-Stand and 150 µl of Wash Solution 1 were added. The beads were resuspended until obtaining a homogenised mix. This step was repeated with Wash Buffer 2. The samples were shaken during 2 minutes at 1200 rpm with open lid in order to dry the beads, avoiding carry out of isopropanol.

Afterwards, 50 µl of TURBO DNase solution (previously prepared) were added, the beads were resuspended until obtaining a homogenised mix and shaken during 15 minutes at 1100 rpm. Then, 50 µl of Rebinding Buffer and 100 µl of isopropanol were added to the sample and it was agitated during 5 minutes at 900 rpm. The tube was again placed into the Magnetic-Stand for 5 minutes or until the solution was clear, supernatant was discarded and two washes with Wash Buffer 2 were performed as previously described. The tube was then shaken with open lid in order to dry the beads. Finally, 50 µl of Elution buffer, previously heated at 65°C, were added to the beads and were resuspended. Afterwards, the tube was shaken 2 minutes at 1200 rpm, incubated at 65°C for 5 minutes and shaken again 2 minutes at 1200 rpm. It was placed on the Magnetic-Stand for 3 minutes and RNA was released from the beads and supernatant was collected.

In samples used for data validation, a spike-in control *C. elegans* miR-39 (Qiagen, Hilden, Germany) was added during extraction protocol before the addition of magnetic beads. Following user manual, exogenous spike-in control was reconstituted and diluted until working solution and 3.5 µl were added into each sample.

3.4 RNA quantification.

Total RNA isolation including small RNA was followed by a quantity and quality measurement before downstream steps.

3.4.1 Spectrophotometric method.

RNA quantification was performed by Nanovue (GE Healthcare Life Sciences, UK), spectrophotometer that measures the absorption of light at 260 nm wavelength and applying Lambert-Beer law correlates absorbance with RNA concentration. Before measuring the sample, the instrument was calibrated with the elution solution (in case of RNA from tissue samples, with RNeasy-free water; in case of RNA from blood samples, with elution buffer) and then 2 µl of RNA were loaded into the instrument. Nanovue automatically calculates RNA concentration, $A_{260/280}$ ratio and $A_{260/230}$ ratio. Both ratios are used as purity indicators, where $A_{260/280}$ indicates possible protein contamination and $A_{260/230}$ indicates organic solution contamination. Pure RNA should present both ratios around 2: $A_{260/280}$ ratio from 1.8 and 2. and a $A_{260/230}$ ratio from 2 to 2.2.

3.5 Reverse transcription.

Total RNA including miRNA was reverse transcribed in order to obtain Complementary DNA (cDNA) of a specific small RNA or all miRNA in the sample using two strategies:

3.5.1 Small Nucleolar RNA, C/D box 68 (SNORD68) reverse transcription.

In order to determine the presence of miRNA and small RNAs in the total RNA extracted from myocardial tissue samples and blood samples, SNORD68 was detected by reverse transcription and Real-Time PCR.

250 ng of total RNA was mixed with 1 µl of 10 mM dNTP mix (Life Technologies, Carldbad, CA, USA), 1 µl of 2 µM reverse specific primer (see Table 3, provided by Integrated DNA Technologies, Iowa, USA) and RNeasy-free water to a total volume of 12 µl. It was incubated on a thermal cycler at 65°C for 5 minutes. 4 µl of 5x First Strand Buffer (Invitrogen by ThermoFisher Scientific, Waltham, MA, USA) and 3 µl of RNeasy-free water were added and the mix was incubated again at 42°C for 2 minutes. Finally, 1 µl of SuperScript III Reverse Transcriptase (200U/µl) (Invitrogen by ThermoFisher Scientific, Waltham, MA, USA) was added and mixed by pipetting. The reaction mix was incubated at 42°C for 50 minutes, followed by enzyme inactivation at 72°C for 15 minutes.

3.5.2 Mature miRNA reverse transcription.

Using miScript II RT Kit (Qiagen, Hilden, Germany), 100 ng of total RNA were mixed with 4 µl of 5x miScript HiSpec Buffer (Qiagen, Hilden, Germany), 2 µl of 10x miScript Nucleics Mix (Qiagen, Hilden, Germany) and 2 µl of miScript Reverse Transcriptase Mix (Qiagen, Hilden, Germany). Volume was adjusted to 20 µl with RNeasy-free water. The reaction mix was incubated at 37°C for 60 minutes and then at 60°C for 5 minutes in a thermal cycler. cDNA was subsequently diluted adding 200 µl of RNeasy-free water.

Specifically, only mature miRNA, certain small nucleolar RNAs and small nuclear RNAs are selectively converted into cDNA thanks to 5x miScript HiSpec Buffer. Mature miRNAs are polyadenylated by poly(A) polymerase and reverse transcribed into cDNA using oligo-dT primers. The oligo-dT primers have a 3' degenerate anchor and a

universal tag sequence on the 5' end, allowing amplification of mature miRNA in the next steps.

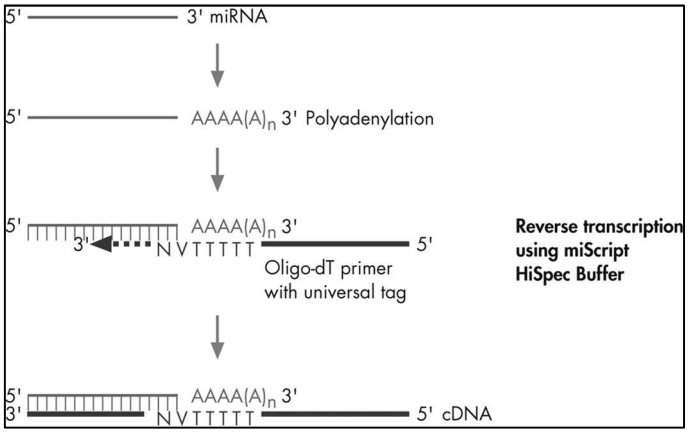

Figure 10: Schematic figure of polyadenylation and reverse transcription mechanism (modified from miScript PCR System Handbook, Qiagen).

3.6 Real-Time PCR (qPCR).

cDNA prepared in reverse transcription step was detected by qPCR using Light Cycler 480 II instrument (Roche, Mannheim, Germany) and SYBR Green I technology. For the detection of SNORD68, specific forward and reverse primers were designed and used (see Table 3 provided by Integrated DNA Technologies, Iowa, USA). Instead, for the detection of mature miRNAs, two strategies were performed.

First, miRNA amplification was performed by miScript PCR array (Qiagen, Hilden, Germany); afterwards, amplification of single miRNAs was carried out by miRNA single assay with specific forward primers (see Table 3, provided by Integrated DNA Technologies, Iowa, USA).

All of three amplification strategies were based on SYBR Green I dye, an asymmetrical cyanine dye that binds to double-stranded DNA (dsDNA) resulting in a complex DNA-dye. The complex absorbs blue light (λ=497 nm) and emits green light (λ=520 nm). During qPCR, SYBR Green I binds every new copy of DNA, resulting in an increase of

fluorescence due to the increase of the number of copies of DNA that is being amplified. In this way, Ct values are acquired.

In addition, melting temperature curve analysis was performed after PCR cycling. It is an assessment of the dissociation-characteristics of double-stranded DNA. As the temperature is raised, the double strand begins to dissociate leading to a rise in the fluorescence. The temperature at which 50% of DNA is denatured is known as Melting Temperature (Tm), and it is characteristic of the sequence of the amplicon. If PCR runs properly, there should be only one melting peak, indicating that only one PCR product has been amplified.

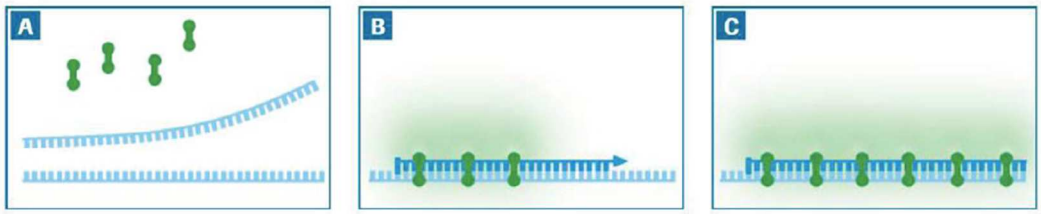

Figure 11: Schematic representation of SYBR Green I. A) Sybr Green I dye only fluorescence when it is bound to dsDNA and excited by blue light. B) As dsDNA is synthesized, SYBR Green I binds the dsDNS and fluorescence signal increases. C) At the end of elongation phase, all DNA is double-stranded, the maximum amount of SYBR Green I is bound and fluorescent signal is maximum. Therefore, the fluorescent signals from SYBR Green I are measured at the end of each elongation phase (modified from http://lifescience.roche.com)

3.6.1 qPCR: detection of SNORD68.

The reaction mix was prepared in a final volume of 20 µl with 10 µl of 1x Master SYBR Green I (Roche, Mannhein, Germany), 0,5 µl of 10 µM specific forward primer (SNORD68-F), 0,5 µl of 10 µM specific reverse primer (SNORD68-R) (see Table 3, provided by Integrated DNA Technologies, Iowa, USA) and 5 µl of RNeasy-free water. 5 µl of SNORD68 cDNA were added to each reaction well. The amplification was carried out under the following conditions: an initial preincubation step at 95°C for 5 minutes; followed by 55 cycles of denaturation at 95°C for 10 seconds, annealing step at 62°C for 20 seconds and extension at 72°C for 10 seconds, where fluorescence was acquired. Melting curve was performed in 1 cycle (95°C for 5 seconds, 65°C for 1

minute and 95°C with continuous acquisition of fluorescence) in order to acquired Melting Temperature Curve (Tm curve). qPCR experiments were performed in duplicate and included a negative control. Ct values were automatically calculated by LightCycler 480 software using second derivative maximum.

qPCR of SNORD68 was carried out only in order to determine the presence of this small nucleolar RNA in the extracts and not in order to quantify it, so relative quantification was not performed with SNORD68 Ct values.

3.6.2 qPCR: detection of miRTC.

In order to determine purity and lack of inhibitors in the samples after reverse transcription, miRNA Reverse Transcription Control RNA (miRTC) was assessed in every sample prior to their use with miScript miRNA PCR Array (Qiagen, Hilden, Germany). The miRTC miScript Primer assesses the performance of the reverse-transcription reaction using the miScript II RT Kit by detecting template synthesized from the kit's built-in miRTC. This control monitors for any variables that may inhibit the reverse transcription reaction.

The lyophilized primer was reconstituted adding 550 µl of RNease-free water. Afterwards, reaction mix for one well was prepared as follows: 12,5 µl of 2x QuantiTect SYBR Green PCR Master Mix (Qiagen, Hilden, Germany) 2,5 µl of 10x miScript Universal Primer (Qiagen, Hilden, Germany), 2,5 µl of 10x miRTC Primer (Qiagen, Hilden, Germany), and 6,5 µl of RNase-free water. The reaction mix was prepared based on the number of samples. After mixing by pipetting, reaction mix was dispensed into the plate and 1 µl of cDNA (previously prepared with miScript II RT Kit) was added on each well.

PCR cycling conditions were: an initial step at 95°C for 15 minutes where DNA polymerase is activated; 45 cycles of 3 steps, denaturation at 95°C for 15 seconds, annealing at 55°C for 30 seconds and extension at 70°C for 30 seconds (fluorescence

data collection). The final step consists in the melting temperature curve: 1 cycle with two steps, 60°C al 15 seconds with a ramp rate of 2,5°C/s and 95°C with continuous acquisition mode (ramp rate 0,03°C/s). During this step, melting temperature curve is acquired. In order to determine if cDNA had no inhibitors and reverse transcription reaction was perfectly performed, Ct values of miRTC should vary between 22 and 26. Instead, melting temperature should be 75,5°C - 75,8°C.

3.6.3 qPCR: miScript miRNA PCR Array.

qPCR of cDNA of mature miRNA (obtained by miScript II RT kit) was performed by miScript miRNA PCR Array, in particular, the pathway focused array of Human Cardiovascular Diseases. 84 miRNAs already correlated with cardiovascular diseases are revealed with this array, in addition to 6 endogenous controls and 2 internal controls.

miScript PCR Controls are primers designed to quantify a panel of 5 snoRNAs (SNORD61, SNORD68, SNORD72, SNORD95, and SNORD96A) and the snRNA RNU6B (RNU6-2). In addition, these small RNAs have been verified to present relatively stable expression levels across tissues and cell types. As a result, miScript PCR Controls serve as normalization controls for relative quantification using the miScript PCR System. All the controls have amplification efficiencies close to 100%.

In addition, two internal controls are present in the array. The miRTC miScript Primer Assay (explained before) and the positive PCR control (PPC). PPC wells contain a predispensed artificial DNA sequence and the assay that detects it. This control monitors for any variables that may inhibit the PCR reaction.

Furthermore, an assay for an exogenous control is also present in the plate. The miScript Primer Assay for *C. elegans* miR-39 detects the miRNeasy Serum/Plasma Spike-In Control, also called Syn-cel-miR-39 miScript miRNA Mimic, which is a *C. elegans* miR-39 mimic. This mimic can be added to the samples, particularly serum or

plasma samples, to control for variations during the preparation of total RNA and subsequent steps. After purification, qPCR detection of the miRNeasy Serum/Plasma Spike-In Control can be performed and these results can then be used for normalization of qPCR results for endogenous miRNAs in the sample. Cel-miR-39 was not added to blood samples analysed with the arrays, but it was detected during validation experiments in order to normalized Ct values.

The design of the array is represented in the table 2.

	1	2	3	4	5	6	7	8	9	10	11	12
A	hsa-let-7a-5p	hsa-let-7b-5p	hsa-let-7c	hsa-let-7d-5p	hsa-let-7e-5p	hsa-let-7f-5p	hsa-miR-1	hsa-miR-100-5p	hsa-miR-103a-3p	hsa-miR-107	hsa-miR-10b-5p	hsa-miR-122-5p
B	hsa-miR-124-3p	hsa-miR-125a-5p	hsa-miR-125b-5p	hsa-miR-126-3p	hsa-miR-130a-3p	hsa-miR-133a	hsa-miR-133b	hsa-miR-140-5p	hsa-miR-142-3p	hsa-miR-143-3p	hsa-miR-144-3p	hsa-miR-145-5p
C	hsa-miR-146a-5p	hsa-miR-149-5p	hsa-miR-150-5p	hsa-miR-155-5p	hsa-miR-15b-5p	hsa-miR-16-5p	hsa-miR-17-5p	hsa-miR-181a-5p	hsa-miR-181b-5p	hsa-miR-182-5p	hsa-miR-183-5p	hsa-miR-185-5p
D	hsa-miR-18b-5p	hsa-miR-195-5p	hsa-miR-199a-5p	hsa-miR-206	hsa-miR-208a	hsa-miR-208b	hsa-miR-21-5p	hsa-miR-210	hsa-miR-214-3p	hsa-miR-22-3p	hsa-miR-221-3p	hsa-miR-222-3p
E	hsa-miR-223-3p	hsa-miR-224-5p	hsa-miR-23a-3p	hsa-miR-23b-3p	hsa-miR-24-3p	hsa-miR-25-3p	hsa-miR-26a-5p	hsa-miR-26b-5p	hsa-miR-27a-3p	hsa-miR-27b-3p	hsa-miR-29a-3p	hsa-miR-29b-3p
F	hsa-miR-29c-3p	hsa-miR-302a-3p	hsa-miR-302b-3p	hsa-miR-30a-5p	hsa-miR-30c-5p	hsa-miR-30d-5p	hsa-miR-30e-5p	hsa-miR-31-5p	hsa-miR-320a	hsa-miR-328	hsa-miR-342-3p	hsa-miR-365a-3p
G	hsa-miR-378a-3p	hsa-miR-423-3p	hsa-miR-424-5p	hsa-miR-451a	hsa-miR-486-5p	hsa-miR-494	hsa-miR-499a-5p	hsa-miR-7-5p	hsa-miR-92a-3p	hsa-miR-93-5p	hsa-miR-98-5p	hsa-miR-99a-5p
H	cel-miR-39-3p	cel-miR-39-3p	SNORD61	SNORD68	SNORD72	SNORD95	SNORD96A	RNU6-2	miRTC	miRTC	PPC	PPC

Table 2: miScript miRNA PCR Array Human Cardiovascular disease design (from https://www.qiagen.com).

Each sample was tested with one miScript PCR array and the mix was prepared considering all 96 wells. In addition, the samples were directly added into the mix. 1375 µl of 2x QuantiTect SYBR Green PCR Master Mix (Qiagen, Hilden, Germany) were mixed with 275 µl of 10x miScript Universal Primer (Qiagen, Hilden, Germany), 1000 µl of RNase-free water (Qiagen, Hilden, Germany) and 100 µl of template cDNA, mixed by pipetting. Afterwards, 25 µl of reaction mix was dispensed to each well of the miScript miRNA PCR array.

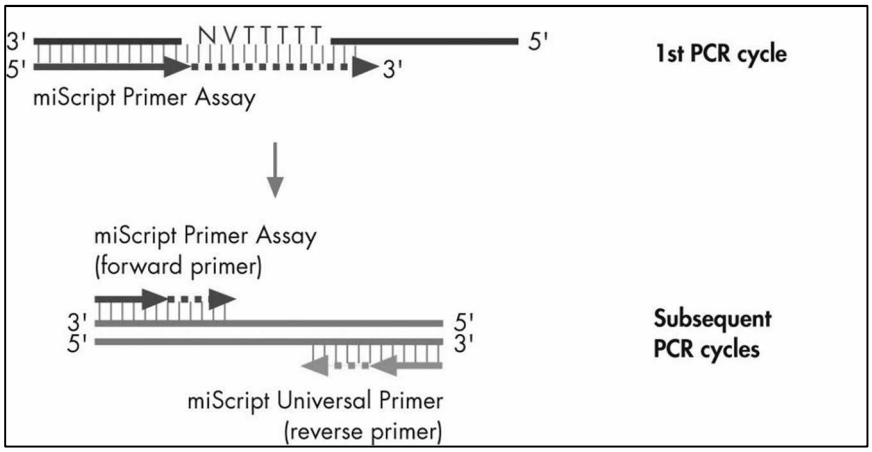

Figure 12: Schematic figure of amplification by qPCR. miScript primer assay is specific for every miRNA. miScript Universal Primer is a universal primer complement to "universal tag" added during reverse transcription step and it is used as reverse primer for all miRNAs. (modified from miScript PCR System Handbook, Qiagen).

Cycling conditions for qPCR were as follows: an initial PCR activation step at 95°C for 15 minutes where DNA polymerase is activated, 45 cycles of 3 steps, denaturation at 95°C for 15 seconds, annealing at 55°C for 30 seconds and extension at 70°C for 30 seconds (fluorescence data collection). The final step consists in the melting temperature curve: 1 cycle with two steps, 60°C al 15 seconds with a ramp rate of 2,5°C/s and 95°C with continuous acquisition mode (ramp rate 0,03°C/s). During this step, melting temperature curve is acquired.

3.6.4 qPCR: single miRNA assay.

Data validation was performed analysing: hsa-miR-21-5p, hsa-miR-144-3p, hsa-miR-155-5p, hsa-miR-122-5p, hsa-miR-208a-3p, hsa-miR-494-3p and hsa-miR-320a. Forward primers for hsa-miR-21-5p, hsa-miR-144-3p, hsa-miR-155-5p, hsa-miR-122-5p, hsa-miR-208a-3p, hsa-miR-494-3p were designed for each mature miRNA as detailed in table 3 and reconstituted the lyophilized primer with RNase-free water at a concentration of 100 µM (Integrated DNA Technologies, Iowa, USA). Hsa-miR-320a was instead detected using miScript primer assay, specific for this mature miRNA (Qiagen, Hilden, Germany).

Reaction mix was prepared as follows (quantity for 1 reaction): 12,5 µl of 2x QuantiTect SYBR Green PCR Master Mix (Qiagen, Hilden, Germany), 2,5 µl of 10x miScript Universal Primer (Qiagen, Hilden, Germany), 2,5 µl of 3 µM of forward primer, final concentration of 0,3 µM/reaction (see Table 3, provided by Integrated DNA Technologies, Iowa, USA) and 6,5 µl of RNase-free water. The reaction mix was prepared based on the number of samples. After mixing by pipetting, 24 µl of the reaction mix was dispensed into the plate and 1 µl of cDNA (previously prepared with miScript II RT Kit) was added on each well. Cycling conditions were the same as used for miScript miRNA PCR array: an initial PCR activation step at 95°C for 15 minutes where DNA polymerase is activated, 45 cycles of 3 steps, denaturation at 95°C for 15 seconds, annealing at 55°C for 30 seconds and extension at 70°C for 30 seconds (fluorescence data collection). The final step consists in the melting temperature curve: 1 cycle with two steps, 60°C al 15 seconds with a ramp rate of 2,5°C/s and 95°C with continuous acquisition mode (ramp rate 0,03°C/s). During this step, melting temperature curve is acquired.

In addition, *C. elegans* miR-39 spike-in control was also detected using miScript primer assay for cel-miR-39 (Qiagen, Hilden, Germany). Mix preparation was performed as

explained before adding 2,5 µl of the specific primer and qPCR running conditions are the same.

3.7 Primer design.

3.7.1 SNORD68.

In order to determine the presence of SNORD68 in extracted samples, two oligonucleotides (forward and reverse) were designed. It was used Primer3web (http://primer3.ut.ee/) (Rozen and Skaletsky, 2000) software to design primers. The input was the transcript sequence of 84 pb of SNORD68 from NCBI (https://www.ncbi.nlm.nih.gov/). The "best" pair of primers was then analysed using BLAST (https://blast.ncbi.nlm.nih.gov/Blast.cgi) and BLAT (https://genome.ucsc.edu), in order to study their specific annealing on the target and not in other parts of RNA or genome. To confirm the amplicon length and Tm, they were also checked by *in silico* PCR tool of UCSC website (http://genomeeuro.ucsc.edu/index.html). Primers were then provided by IDT (Integrated DNA Technologies, Iowa, USA).

3.7.2 Mature miRNA.

The oligonucleotide primers used for the validation of selected miRNA were designed by the software miRprimer (Busk, 2014). It is based on miR-specific RT-qPCR method and designed primers are able to perform well on targets in complex biological samples yielding typical qPCR amplification curves, melting curves with a single peak and amplification efficiencies close to 100%. As qPCR performed in the arrays consists on poly-adenilation of mature miRNA, adding an universal tag to use as reverse primer, the design was only carried out for the forward primer.

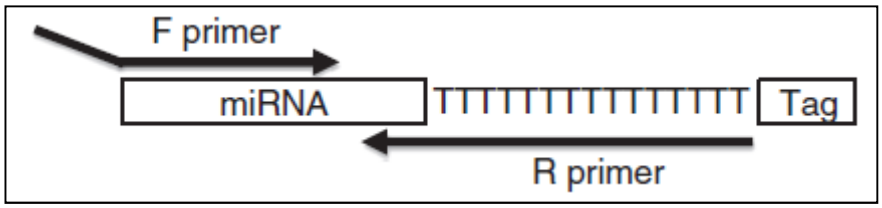

Figure 13: Schematic representation of forward and reverse primers (modified from Busk 2014).

The design of the forward primer with this tool consisted on finding the best possible 3'-end sequence, complement almost the whole length of mature miRNA and elongated it until get a melting temperature of 55°C -59°C. Primers were assigned a score according to some parameters such as the sequence of the 2-5 nucleotides closest to the 3'-end, length of the miR-specific part of the primer and putative secondary structures. Instead of using the same software to design also reverse primers, Universal miScript Primer (Qiagen, Hilden, Germany) was used as reverse primer.

Taking this into consideration, forward primers were then analysed in order to determine which one matches better the following characteristics: melting temperature of approximately 55°C (annealing temperature of universal primer) and specific complementarity with target miRNA, not targeting also other members of the same family or other parts of the genome. Primers were analysed using different bioinformatics tools in order to check their reaction specificity and accuracy. They were aligned by miRBase (http://www.mirbase.org) on mature human miRNA and BLAT (https://genome.ucsc.edu) on genome reference sequence in order to verify their specificity annealing and to avoid the possibility of binding another mature miRNAs. Primers were then provided by IDT (Integrated DNA Technologies, Iowa, USA). Primer sequences, length and melting temperature are listed in Table 3.

Target	Sequence (5'-3')	Length (pb)	Tm (melting temperature)
SNORD68-F	CGCGTGATGACATTCTCC	18	53.5
SNORD68-R	GATGGAAAAGGGTTCAAATGT	21	51.2
hsa-miR-122-5p	CGCTGGAGTGTGACAATGG	19	56.3
hsa-miR-144-5p	CGCAGGGATATCATCATATACTGT	24	54
hsa-miR-155-5p	CGCAGTTAATGCTAATCGTGATAG	24	53.8
hsa-miR-208a-3p	CGCAGATAAGACGAGCA	17	51.8
hsa-miR-21-5p	GCAGTAGCTTATCAGACTGATG	22	52.9
hsa-miR-494-3p	CAGTGAAACATACACGGGAA	20	52.3

Table 3: List of primers with sequences, length and Tm.

3.8 Agarose gel.

After qPCR, amplicons were analysed by running amplification products in agarose gel in order to confirm that only one target was amplified by observing only one band. 4% agarose gel was produced by adding 4 g of agarose in 100 ml of 1X Tris-Acetate-EDTA (TAE) buffer. The solution was heated in a microwave to dissolve agarose and 5 µl of Nancy-520 DMA Gel Stain (Sigma-Aldrich, Saint Louis, MO, USA) were added. It was cast in a sealed tray and a proper comb was inserted. 5 µl of PCR products were mixed with 2 µl of OrangeG 6X (AB Analitica, Padua, Italy) and then loaded into each gel well. In addition, 5 µl of pUC19/MspI DNA Marker (AB Analitica, Padua, Italy) were loaded in order to determine the fragment size. Electrophoretic run was performed at 100 µl in 1X TAE buffer. Visualization was achieved on a LAS mini 4000 (Fujifilm, Tokyo, Japan). When only one target was amplified, only one band was observed on the gel, between 70 to 80 nt length.

3.9 Data analysis: relative quantification

Ct values collection was performed using Second Derivative Maximum analysis method available in LightCycler 480 software (Roche, Mannhein, Germany). It is an algorithm based on the kinetics of a PCR reaction that identifies the crossing point (Cp) of a reaction as the point where the reaction's fluorescence reaches the maximum of the second derivative of the amplification curve, which corresponds to the poring where the acceleration of the fluorescence signal is at its maximum. The advantage of this method is that produces consistent results. In addition, Melting Temperature Analysis was also performed with LightCycler 480 software (Roche, Mannhein, Germany). When PCR runs properly, only one melting peak is observed for each miRNA analysed on each sample.

Raw Ct values were analysed using ΔΔCt Method of Relative Quantification. It determines the differences in the expression level of a specific miRNA between samples from AC group in comparison with HC. It is expressed in fold-change, meaning how many times a miRNA is more/less expressed in the AC group in comparison with HC, and also in terms of fold-regulation. A miRNA is considered significantly overexpressed when fold-change value is greater than 2. Instead, it is considered underexpressed when its fold-change is lower than 0,5. Fold-regulation represents fold-change in a biologically meaningful way, where value of fold-regulation is equal to fold-change value when is greater than one, indicating an up-regulation. Instead, when fold-change value is less than one, fold-regulation is the negative inverse of fold-change, indication down-regulation. In this case, a miRNA is significantly upregulated when fold-regulation is greater than 2 and downregulated when fold-regulation is lower than -2. Expression levels of miRNAs of every sample are first normalized based on an endogenous control, Ct mean of the whole array or an exogenous control; depending on the experiment.

$$Normalization: \Delta Ct_{miRNA\ in\ a\ sample} = Ct_{miRNA} - Ct_{normalizer}$$

$$\Delta\Delta Ct = \Delta Ct_{AC-sample} - \Delta Ct_{Control}$$

$$Fold - change = 2^{-\Delta\Delta Ct}$$

$$Fold - change > 1 \rightarrow Fold - regulation = Fold - change$$

$$Fold - change < 1 \rightarrow Fold - regulation = -\frac{1}{Fold - change}$$

Figure 14: Relative-quantification formula.

3.9.1 SNORD68 data analysis.

In order to determine the presence of SNORD68, and as a consequence, determine that miRNA isolation worked properly, Ct values were considered in a "qualitative analysis", where the value should be lower than 35 (cut-off) and only one melting peak should be observed.

3.9.2 miScript miRNA PCR array: data analysis.

Ct values were collected as explained before, by performing Second Derivative Maximum analysis (software LC480 Roche). Raw Ct values were then analysed using Data Analysis Center by Relative Quantification (http://www.qiagen.com/it/shop/genes-and-pathways/data-analysis-center-overview-page/). Data were loaded into the software in an excel file with all Ct values of every sample. Ct cut-off was set at 35, so Ct values greater than 35 or non-detected were automatically changed to 35. Afterwards, Ct values of both positive controls, PPC and miRTC were examined. If RNA samples were of high quality and the cycling program run correctly, the Ct value

of PPC should be 19±2. Ct values of the miRTC were examined using the values for the PPC by calculating ΔCt between Ct average of miRTC and Ct average of PPC.

$$\Delta\mathrm{Ct} = \mathrm{AVG}\ Ct^{miRTC} - AVG\ Ct^{PPC}$$

Figure 15: miRTC formula (quality control sample determination).

If this value was less than 7, then no inhibition of the reverse-transcription reaction was apparent and the sample could be subsequently analysed. If this value was greater than 7, there was evidence of impurities that may have inhibited the reverse transcription reaction. In this case, sample could not be considered for further analysis.

Once samples passed "quality control", normalization was performed. For each miRNA of each sample, Ct values were normalized using Global Ct Mean of expressed miRNAs Method. This method automatically calculates a global Ct mean for the miRNA targets that are commonly expressed in all samples being analysed. Afterwards, values were analysed using relative quantification with the formulas explained before. Output file collected this information as well as fold-change and fold-regulation values. Values coloured in red indicated up-regulation and values coloured in blue indicated down-regulation. In addition, AC-samples were also considered as a unique group and after normalization, average of ΔCt (normalized Ct) was considered for the relative quantification analysis obtaining fold-change and fold-regulation of the entire AC-group.

3.9.3 miRNA validation: data analysis

Data analysis of Ct values obtained for the validated miRNAs on the 50 blood samples (42 AC-subjects and 8 HC) was performed also with ΔΔCt relative quantification method. In this case, *C. elegans* miR-39 spike-in control was considered for normalization and Ct values were normalized with the average of Ct values of cel-miR-39 for each sample. *C. elegans* miR-39 spike-in control is an exogenous small RNA,

without homologies inside human RNAs, that is used for sample-to-sample normalization of RNA at recovery, reverse transcription and amplification levels.

Following relative quantification formulas explained before, data analysis was performed considering the 42 AC-samples separately and considering the 42 AC-sample as a unique group. In both cases, they were analysed in comparison with HC.

3.10 *In silico* target prediction

In order to determine possible targets of differentially expressed miRNAs observed in AC affected subjects, a prediction *in silico* was performed using DIANA-mirPath.v.3 (Vlachos et al. 2015). It consists in a web-server that provides accurate statistics for predicted miRNA targets based on experimentally validated miRNA interactions derived from the database DIANA-Tarbase. Subsequently, pathways significantly enriched with genes belonging the union of targeted genes of differentially expressed miRNA are identified. In this way, dysregulated miRNAs were loaded in the software that calculates possible target-genes and the union of these targets were then processed by KEGG analysis. The result consisted in a list of possible pathways in which differentially expressed miRNAs were involved where the number of miRNA and the list of genes were specified. In addition, a p-value was also calculated determining the best pathway with the lower p-value (http://snf-515788.vm.okeanos.grnet.gr/).

3.11 ROC curve analysis

The diagnostic performance of the miRNAs and the accuracy of miRNA levels (variable) to discriminate AC from HC cases was evaluated using Receiver Operating Characteristic (ROC) curve analysis using MedCalc Statistical Software version 17.9.4 (MedCalc Software bvba, Ostend, Belgium; http://www.medcalc.org; 2017). In a ROC curve, the true positive rate (Sensitivity) is plotted in function of the false positive rate (100-

Specificity) for different cut-off points. Each point on the ROC curve represents a sensitivity/specificity pair corresponding to a particular decision threshold. A test with perfect discrimination (no overlap in the two distributions) has a ROC curve that passes through the upper left corner (100% sensitivity, 100% specificity). Therefore, the closer the ROC curve is to the upper left corner, the higher the overall accuracy of the test (Zweig and Campbell 1993).

Fold-change values for miRNA of interest were loaded into the software, dividing them in AC affected group (diagnosis=1) and healthy group (diagnosis=0). The method DeLong was used for the calculation of the standard error of the area under the curve (DeLong et al., 1988). The result was the Area Under the ROC curve (AUC) value with a standard error and 95% of Confidence Interval. When the variable cannot distinguish between the two groups (meaning it has no diagnostic significance), the area will be equal to 0,5; instead, when there is a perfect separation of the values of the two groups (meaning the test can diagnose significantly affected from healthy subjects), the area under the ROC curve equals 1. In addition, the p-value was calculated, and if it is smaller than 0,05, then it can be concluded that AUC can significantly distinguish both groups.

4 RESULTS

4.1 Meta-analysis: role of miRNA in cardiomyopathies.

In order to investigate whether expression profile of miRNA was previously studied in primary cardiomyopathies, a meta-analysis has been carried out, in which we focused on three primary cardiomyopathies: HCM, DCM and AC.

4.1.1 Hypertrophic Cardiomyopathy.

HCM is the most common primary cardiomyopathy (1:500 in the general population) that presents heterogeneous clinical and genetic characteristics (Maron et al., 2006). Mutations mainly occur in genes encoding cardiac contractile apparatus (Maron et al., 2014) and are inherited as an autosomal dominant trait. Among them, 70% are found in sarcomere genes cardiac b-myosin heavy chain (*MYH7*) and cardiac myosin binding protein C (*MYBPC3*). HCM presents morphological and pathological heterogeneity, penetrance and age dependency with the consequence of diverse clinical outcomes with conditions going between asymptomatic patients to cardiac arrhythmias and sudden cardiac death (Spirito et al., 2014). A high percentage of patients are asymptomatic or mildly asymptomatic and diagnosis is made during family screening or by incidental observation in middle or late adulthood where functional debility of the heart is already progressed. The management of HCM sometimes results hardly understandable because there is not always a correlation between genotype and phenotype, in addition family members with the same mutation develop distinct symptoms (Maron et al., 2014). To this regard, transcriptional profile modified by miRNAs expression and another posttranscriptional modifications seem to be crucial to understand the onset of HCM.

Hypertrophic growth of cardiomyocytes has been studied by van Rooij and colleagues where they analysed 186 miRNAs. They described more than 12 miRNAs that are

differentially expressed in hypertrophic or failing hearts derived from mice and humans, discovering a stress-responsive miRNA, hsa-miR-195. Its overexpression in transgenic mice resulted in pathological cardiac remodelling and HF (van Rooij et al., 2006).

In a small study, 370 miRNAs were analysed in pathological HCM tissue, with and without MYH7 mutation. Two miRNAs (hsa-miR-590-5p and hsa-miR-92a) were overexpressed in HCM patients in comparison with healthy control, but only hsa-miR-495 expression was different between HCM-mutated and HCM-non-mutated tissues (Palacín et al., 2011). In addition, the same group studied the profile expression of miRNA in plasma samples of patients affected by HCM, where 10 miRNAs were analysed in 24 patients and compared to healthy controls. Only hsa-miR-483-5p was overexpressed among HCM patients (Palacín et al., 2013).

One of the most frequent affected genes in HCM is MYBPC3, which encodes the thick filament protein cardiac myosin binding protein C. Kuster and colleagues studied profile expression of miRNAs in 6 patients with a loss-of-function mutation in MYBPC3. Among 699 miRNAs analysed, 13 of them formed a miRNA signature unique for HCM: 10 were upregulated (hsa-miR-181-a2, hsa-miR-184, hsa-miR-497, hsa-miR-204, hsa-miR-222, hsa-miR-96, hsa-miR-34b, hsa-miR- 383, hsa-miR-708 and hsa-miR-371-3p) and 3 were downregulated (hsa-miR-10b, hsa-miR-10a and hsa-miR-10b*). *In silico* studies demonstrated that a large number of genes regulated by differentially expressed miRNAs were associated with cardiac hypertrophic signaling pathway where a large number of predicted mRNA target was involved in b-adrenergic signaling (Kuster et al., 2013).

Myocardial interstitial fibrosis is a common and early feature of HCM. Fang and colleagues studied circulating miRNAs as biomarkers of diffuse myocardial fibrosis in HCM patients. Among 84 miRNAs, plasma levels of 14 miRNAs were significantly increased in patients with diffuse fibrosis compare to healthy controls. They validated 12 miRNAs (hsa-miR-18a-5p, hsa-miR-146a-5p, hsa-miR-30d-5p, hsa-miR-17-5p, hsa-

miR-200a-3p, hsa-miR-19b-3p, hsa-mir-21-5p, hsa-miR193a-5p, hsa-miR-10b-5p, hsa-miR-15a-5p, hsa-miR-192-5p, hsa-miR-296-5p, hsa-miR-96-5p and hsa-miR-373-3p) as potential biomarkers with moderate predictive values in order to differentiate 2 subgroups of HCM patients, with or without diffuse myocardial fibrosis, and the control group, suggesting miRNAs as reliable, accessible and disease-specific biomarkers of diffuse fibrosis in HCM (Fang et al., 2015).

Different clinical aspects of HCM lead to a subclassification of the disease into hypertrophic non-obstructive (HNMC) and obstructive cardiomyopathy (HOCM). An analysis of miRNA that play a significance role in cardiac remodelling in HNMC, HOCM, cardiac amyloidosis and aortic stenosis (AS) patients was perform in serum samples. There were significantly differences between miR-29 family and hsa-miR-155 among the four groups. Hsa-miR-29a was only significantly upregulated in HOCM group and not in HNMC whereas hsa-miR-29c was upregulated in AS patients. In contrast, hsa-miR-155 was downregulated only in both groups of HCM patients compared to AS and cardiac amyloidosis patients (Derda et al., 2015).

Other authors attempt to assess circulating levels of 21 miRNAs in HCM patients finding 8 of the 21 miRNAs specific for the HCM group by ROC curve analysis. Three of them (hsa-miR-27a, hsa-miR-29a and hsa-miR-199a-5p) were significantly upregulated in the HCM group and correlated with left ventricular mass. Among them, only hsa-miR-29a was correlated also with the extension of myocardial fibrosis identifying hsa-miR-29a as potential biomarker for myocardial remodelling assessment in HCM (Roncarati et al., 2014).

4.1.2 Dilated Cardiomyopathy.

DCM is a common and largely irreversible form of heart muscle disease with a prevalence of 1:2500. It may manifest at a wide range of ages and it is usually identified when associated with severe symptoms. DCM is characterized by ventricular

chamber enlargement and systolic dysfunction with normal chamber thickness leading to progressive HF and decline in left-ventricular (LV) contractile function. Approximately 20-35% of cases exhibit a familial inheritance associated with at least 40 genes but with incomplete penetrance (Maron et al., 2006). A wide variety of genes have been associated with DCM, including genes encoding nuclear envelope proteins, sarcomere proteins, structural proteins, ion channels and unclassified proteins (Dellefave and McNally 2010). The identification of genetic factors that lead to clinical manifestation of the diseases is the key to understand the trigger mechanism that initiates the disorder (Cho et al., 2016).

Wijnen and colleagues investigated the effect of the overexpression of miR-30c in a mouse model. They showed how the cardiomyocyte-specific overexpression of mmu-miR-30c leads to DCM, correlating the onset of the disease with the level of mmu-miR-30c overexpression (Wijnen et al., 2014).

Another study, in which 3100 miRNAs were assessed in plasma of 4 DCM patients showed 47 were differentially expressed compared to 3 healthy subjects. They chose 3 miRNAs (hsa-miR-3135b, hsa-miR-3908 and hsa-miR-5571-5p) as possible biomarkers of the disease as their levels were significantly increased in plasma samples. They confirmed these results in a larger cohort and revealed that overexpression of hsa-miR-3135b, hsa-miR-3908 and hsa-miR-5571-5p had discriminatory power to distinguish DCM patients from controls by ROC curve analysis (Wang et al., 2017).

Levels of a circulating miRNA in plasma, hsa-miR-185, were assessed in patients with DCM comparing to healthy controls not only at the moment of DCM diagnosis but also after one-year follow-up. In this study, expression of hsa-miR-185 was significantly higher in DCM patients but no correlation between hsa-miR-185 and cardiac function at baseline was found. Most of DCM patients were divided into two groups based on cluster distribution of hsa-miR-185, high group and low group. After 1-year follow-up

period, during which patients underwent standard therapy, circulation levels of hsa-miR-185 were stable, but the high-group demonstrated apparent improvements in left ventricular size and systolic function with significant decline in cardiovascular mortality. This indicated that higher hsa-miR-185 levels in circulation caused better clinical outcome of DCM patients, suggesting hsa-miR-185 as novel biomarker for DCM clinical outcome (Yu et al., 2011).

A different strategy to analyse circulating miRNAs is to reveal miRNAs expression in peripheral mononuclear cells (PBMCs), instead of using plasma or serum, avoiding the question of miRNA origin tissue. Some studies argue how PBMCs expression profile mirrors pathological profile in the specific tissue (Liew et al., 2006). 3060 miRNAs were studied in 7 DCM patients and 7 controls by genome-wide miRNA microarray looking for a specific PBMCs signature in DCM patients. This miRNA signature was different from cardiac-signature, but it revealed that all members of miR-548 family were downregulated in DCM samples compared to controls. After confirmation analysis of hsa-miR-548c as possibile biomarker, ROC analysis showed that it had the discriminatory power to differentiate controls and DCM affected patients (Gupta et al., 2014).

Among different mutations discovered in DCM patients, titin (*TTN*) mutations are the leading cause of DCM since 25% of familial cases present mutations in this gene. According to this, Zhou Q and colleagues generated a mouse model with TTN truncation found in a DCM affected family. They observed how levels of mmu-miR-208b were increased during DCM development in mice. miR-208b belongs to the myomiR family together with miR-208a and miR-499 (van Rooij et al., 2009). Constitutively mmu-miR-208b overexpression in cardiomyocytes showed a normal contraction and preserved function, while α-myosin heavy chain (*MYH6*) was downregulated and MYH7 was upregulated, suggesting these two genes as regulatory targets of mmu-miR-208b. Furthermore, miRNA profile was assessed in DCM patients

and hsa-miR-208b was significantly upregulated in DCM compared to ischemic heart disease and myocarditis, suggesting this miRNA as specific for DCM (Zhou et al., 2017).

Fibrosis of the extracellular matrix (ECM) is one of the cardinal features of DCM, which contributes to the development of HF. However, dynamics of collagen metabolism and levels of circulating miRNAs are unknown at the various stages of DCM. Pawel Rubis and colleagues try to correlate miRNA signature and quantity of ECM fibrosis in DCM patients. Patients were divided in four groups based on presence of fibrosis (with or without, new-onset DCM or chronic). Serum levels of hsa-miR-21, hsa-miR-26, hsa-miR-29 and hsa-miR-30 were significantly different between DCM patients and control samples, however no differences were observed among groups. ECM was correlated only with hsa-miR-26; however, collagen volume fraction (a quantitative expression of fibrosis) was correlated with hsa-miR-26 and hsa-miR-30. This provides novel insights into the complexity of fibrosis and DCM (Rubiś et al., 2017).

4.1.3 Arrhythmogenic Cardiomyopathy.

AC is a rare disease (1:2000 – 1:5000) of the heart muscle characterized by a progressive loss of myocytes and fatty or fibro-fatty replacement, producing a progressive dystrophy of the ventricular myocardium and interfering with electrical impulse conduction (Maron et al., 2006).

Its clinically heterogeneity and its incomplete penetrance suggest that other mechanisms, such as epigenetics, contribute together with gene mutations in the development of the disease. Zhang and colleagues studied miRNA profile expression in 24 AC patients compared to controls. They assessed levels of 1078 miRNAs by qRT-PCR, identifying 24 differentially expressed miRNAs in AC samples. Furthermore, they validated these data and also performed ROC curve analysis, in order to determine whether these miRNAs have diagnostic power. The conclusion was that

overexpression of hsa-miR-1251, hsa-miR-21-3p, hsa-miR-21-5p, hsa-miR-212-3p and hsa-miR-34a-5p, and downregulation of hsa-miR-135b, hsa-miR-138-5p, hsa-miR-193-3p, hsa-miR-302b-3p, hsa-miR-302c-3p, hsa-miR338-3p, hsa-miR-491-3p, hsa-miR-575, hsa-miR-4254 and hsa-miR-4643, allowed the discrimination between AC and healthy controls. Among them, hsa-miR-21-5p and hsa-miR-135 may play an important role in the regulation of Wnt/β-catenin and Hippo Signaling pathways resulting in phenotype manifestation of AC (Zhang et al., 2016).

A pathogenic downregulation of miR-184 was observed in PKP2-deficient cells and mouse models of AC by Gurha and colleagues. Low miR-184 levels were associated with upregulation of its target genes, including genes involved in lipid synthesis and enhanced adipogenesis. Indeed, overexpression and knockdown of miR-184 suppressed and enhanced adipogenesis, respectively, in HL-1 cells and cardiac mesenchymal progenitor cells (MPCs). These findings implicated miR-184 in the pathogenesis of excess adipogenesis in PKP2-deficient cells (Gurha et al., 2016).

In a recent study, Sommariva and colleagues have identified hsa-miR-320a as a potential plasmatic biomarker of AC. In the first place, 377 miRNAs were screened in plasma of 3 AC patients and 3 healthy controls (HC). 121 miRNAs were detected in all plasma samples and 5 showed a potential differential expression between AC patients and controls. When these 5 miRNAs were assessed in 36 AC patients and 53 healthy controls, only hsa-miR-320a presented a significantly lower expression. Plasmatic levels of hsa-miR-320a showed 0,53-fold expression difference between AC and healthy control. Furthermore, miRNA expression profile in AC patients was also compared to Idiopathic Ventricular Tachycardia patients (IVT) and hsa-miR-320a showed 0,78-fold less expression, suggesting not only hsa-miR-320a as a potential biomarker for AC patients but also as a potential discriminatory biomarker for AC vs IVT. In addition, plasma levels of hsa-miR-320a were not influenced by intense physical activity, so authors speculated that hsa-miR-320a differential expression is

independent from increased mechanical stretch and training-induced adaptive heart remodelling (Sommariva et al., 2017).

Further, another study included 62 patients with ventricular arrhythmia (VA), where 28 had a definite AC, 11 had a borderline AC and 23 present IVT. Plasma levels of hsa-hsa-miR-144-3p, hsa-miR-145-5p, hsa-miR-185-5p and hsa-miR-494 presented a significant higher expression in AC definite patients with VA compared to borderline AC patients and IVT patients. Indeed, plasma levels of hsa-miR-494 were associated with the recurrence of VA after ablation in definite AC patients (Yamada et al., 2017).

4.2 Cohort

A total number of 59 AC affected subjects were included in this study, from which 39 males and 20 females, age 35±12 (range from 23 to 47). Clinical diagnosis of all subjects was definite according to the 2010 Task Force major and minor criteria (Marcus et al. 2010).

4.3 miRNA isolation and quantification.

Isolation of RNA from tissue samples resulted in 30 µl of eluted total RNA with a concentration of 215±20 ng/µl, $A_{260/280}$ ratio of 2±0.15 and $A_{260/230}$ ratio of 1.5±0.2. Instead, from whole blood, RNA was eluted in 50 µl and mean concentration obtained was 12.9±2.9 ng/µl, with a $A_{260/280}$ ratio of 1.99±0.18 and $A_{260/230}$ ratio of 1.2±0.28.

The high values of $A_{260/280}$ ratio (about 2) in tissue and blood samples demonstrated a proper quality of RNA without protein contaminations. The low $A_{260/230}$ ratio (1.2-1.5), which indicated organic inhibition, did not affect reverse transcription or amplification.

4.4 SNORD68 detection.

Isolated RNA from myocardial tissue and blood samples underwent reverse transcription and Real-Time PCR amplification of SNORD68 with specific forward and reverse primers, previously validated in order to set the concentration and the temperature of annealing to get one melting peak at 79.7 °C and one band on agarose gel of 69 pb, indicating the specific amplification of SNORD68. Detection of this small nucleolar RNA was observed in every sample proving evidence about the proper functioning of isolation protocols and the presence of small RNAs in the extracts.

4.5 miRTC detection.

In order to determine lack of inhibitors in RNA extracts, miRTC assay was performed in every sample assessing the performance of the reverse-transcription reaction detecting a synthetic template. Every sample underwent reverse transcription and amplification, obtaining Ct values between 23 and 26 (Ct mean = 24,8±0,55), indicating proper functioning of reverse transcription and no presence of inhibitors in the samples.

4.6 miRNA expression profile analysis: tissue samples.

miRNA profiling by an 84-miRNA array correlated with cardiovascular diseases on 10 myocardial tissue samples from the RV, 8 from AC affected subjects (3 PKP2, 3 DSP and 2 DSG2) and 2 HC showed a considerable difference of miRNA expression levels between HC and the different AC genotype groups (see Figure 16), where green colour represents low expression and red colour means high expression. It is possible to observe a different colour profile between clustergram lines corresponding with a different miRNA expression profile among AC subjects in comparison with control.

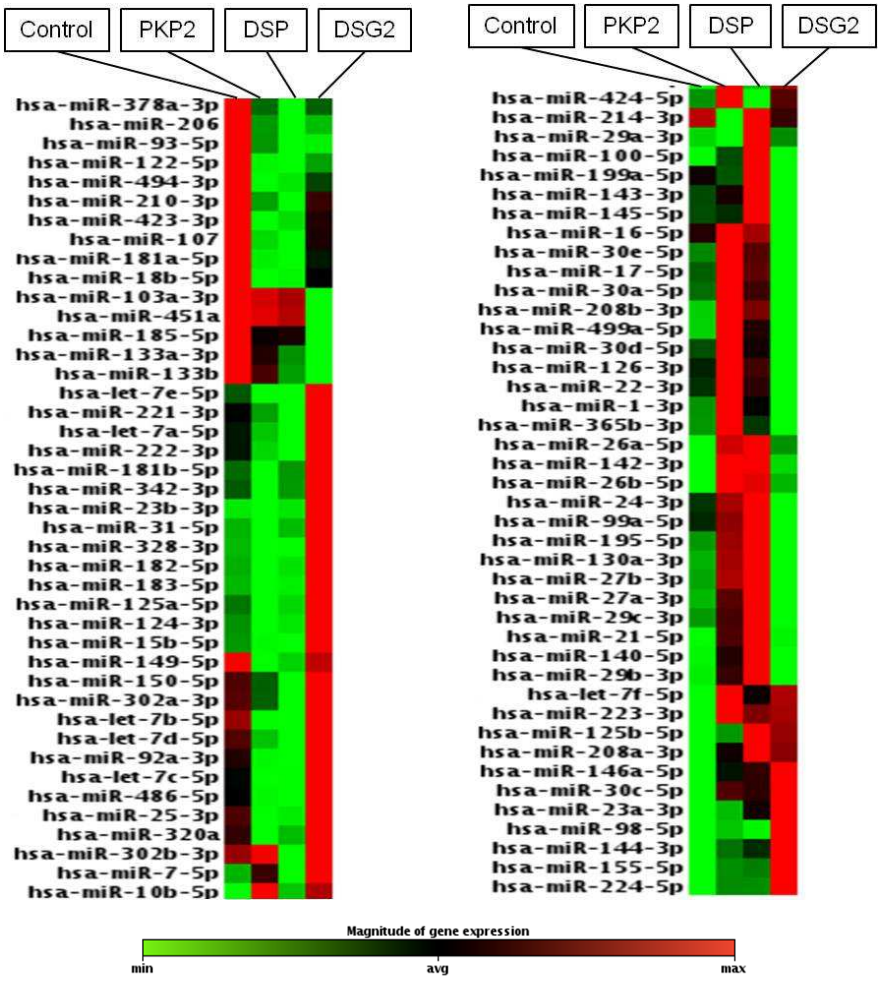

Figure 16: Clustergram representation of the 84-miRNA array of HC, PKP2 group, DSP group and DSG2 group.

4.6.1 Genotype-related profiles.

Analysing in detail this different miRNA expression profile between AC-affected subjects and HC, three different profiles emerged grouping samples based on their demosomal genes. In this way, PKP2-mutation carriers (PKP2 group) displayed 19 differentially expressed miRNAs, 9 overexpressed and 10 underexpressed (PKP2 profile). Subjects with a mutation in DSP gene (DSP group) exhibited 15 differentially expressed miRNAs, 7 overexpressed and 8 underexpressed (DSP profile). Finally, another 14 miRNAs were expressed differently among DSG2 mutation carriers (DSG2

group), 7 overexpressed and 7 underexpressed (DSG2 profile). Differentially expressed miRNA are listed on Table 4.

miRNA differentially expressed in AC subjects vs HC (tissue) divided based on genotype.					
PKP2 - samples		**DSP - samples**		**DSG2 - samples**	
Differentially expressed miRNAs		Differentially expressed miRNAs		Differentially expressed miRNAs	
19		**15**		**14**	
Over	**Under**	**Over**	**Under**	**Over**	**Under**
9	**10**	**7**	**8**	**7**	**7**
Upregulated: hsa-miR-100-5p; hsa-miR-10b-5p; hsa-miR-140-5p; hsa-miR-142-3p; hsa-miR-195-5p; hsa-miR-208b-3p; hsa-miR-21-5p; hsa-miR-27a-3p; hsa-miR-29b-3p.		**Upregulated:** hsa-miR-100-5p; hsa-miR-140-5p, hsa-miR-142-3p; hsa-miR-208b-3p; hsa-miR-21-5p; hsa-miR-27a-3p; hsa-miR-29b-3p.		**Upregulated:** hsa-miR-10b-5p; hsa-miR-125a-3p; hsa-miR-155-5p; hsa-miR-223-3p; hsa-miR-224-5p; hsa-miR-23a-3p; hsa-miR-23b-3p.	
Downregulated: hsa-miR-122-5p; hsa-miR-149-5p; hsa-miR-182-5p; hsa-miR-18b-5p; hsa-miR-320a; hsa-miR-378a-3p; hsa-miR-423-3p; hsa-miR-486-5p; hsa-miR-494-3p; hsa-miR-92a-3p.		**Downregulated:** hsa-miR-122-5p; hsa-miR-149-5p; hsa-miR-18b-5p; hsa-miR-206; hsa-miR-320a; hsa-miR-378a-3p; hsa-miR-486-5p; hsa-miR-494-3p.		**Downregulated:** hsa-miR-1-3p; hsa-miR-133a-3p; hsa-miR-133b; hsa-miR-143-3p; hsa-miR-16-5p; hsa-miR-22-3p; hsa-miR-451a.	

Table 4: miRNA differentially expressed between AC subjects in comparison with HC. It is specified the number and the miRNA differentially expressed divided in based on genotype.

The three different profiles are represented in figures 17-19, where fold-regulation values were calculated by relative quantification in comparison with HC and are plotted on the vertical axis.

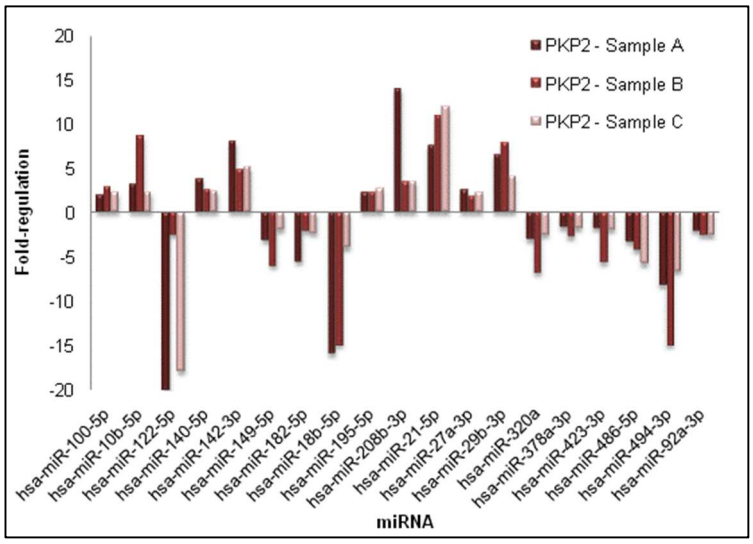

Figure 17: Representation of fold-regulation of differentially expressed miRNAs of PKP2 group.

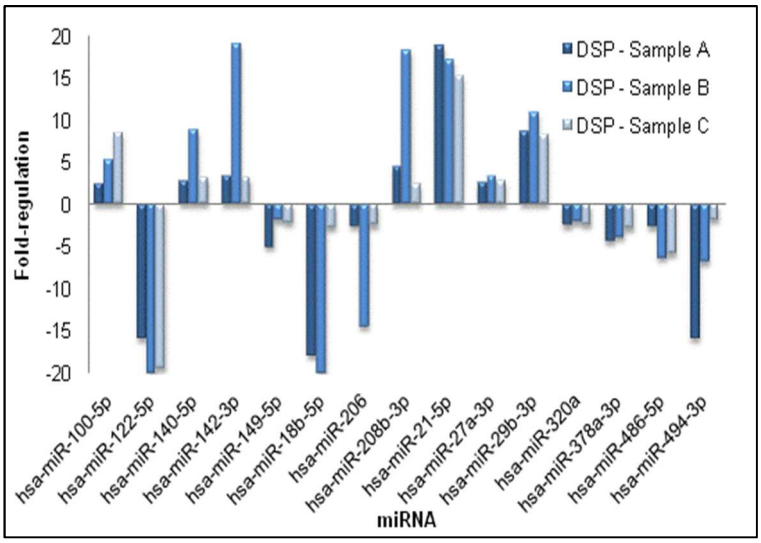

Figure 18: Representation of fold-regulation of differentially expressed miRNAs of DSP group.

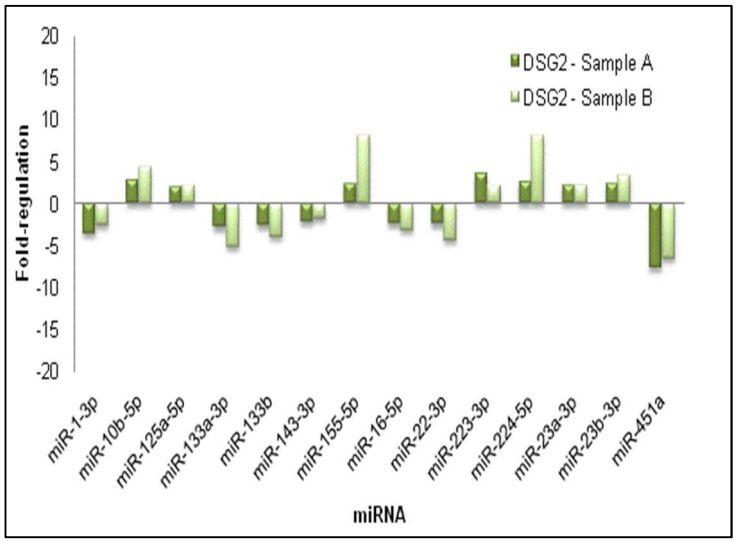

Figure 19: Representation of fold-regulation of differentially expressed miRNAs of DSG2 group

Fold-regulation of differentially expressed miRNAs from the 3 samples of PKP2 group is represented on figure 17; instead, on figure 18 is represented the 3 samples from DSP group and on figure 19, the two samples from DSG2 group. Positive values indicate overexpression and negative values indicate underexpression.

Observing genotype-related miRNA expression profiles in detail, a common miRNA signature was observed between PKP2 and DSP groups. The common profile expression between PKP2 and DSP is depicted in figures 17 and 18, where it is possible to observe a common signature among graphs. Indeed, analysing values of fold-regulation, we identified 14 differentially expressed miRNAs in common between PKP2 and DSP profiles (PKP2/DSP profile). Interestingly, none of them were differentially expressed on DSG2 samples. Among these 14 miRNAs, 7 were overexpressed and 7 were underexpressed, as described in table 5.

PKP2/DSP common differentially expressed miRNAs	
Upregulated (7 miRNAs)	**Downregulated (7 miRNAs)**
hsa-miR-100-5p; hsa-miR-140-5p; hsa-miR-142-3p; hsa-miR-208b-3p; hsa-miR-21-5p; hsa-miR-27a-3p; hsa-miR-29b-3p.	hsa-miR-122-5p; hsa-miR-149-5p; hsa-miR-18b-5p; hsa-miR-320a; hsa-miR-378a-3p; hsa-miR-486-5p; hsa-miR-494-3p.

Table 5: List of Differentially expressed miRNAs in common between PKP2 and DSP groups.

4.6.2 Arrhythmogenic Cardiomyopathy-group profile.

We subsequently analysed all 8 AC tissue samples grouped together, independently from their genotype background, performing relative quantification analysis by using the mean of normalized data of each miRNA among the whole group. We identified 26 differentially expressed miRNAs, either over or under-expressed, in comparison with HC (Figure 20). All 26 differentially expressed miRNAs were present also in the

previous genotype-based profiles, being within the identified miRNA on PKP2/DSP and DSG2 profiles.

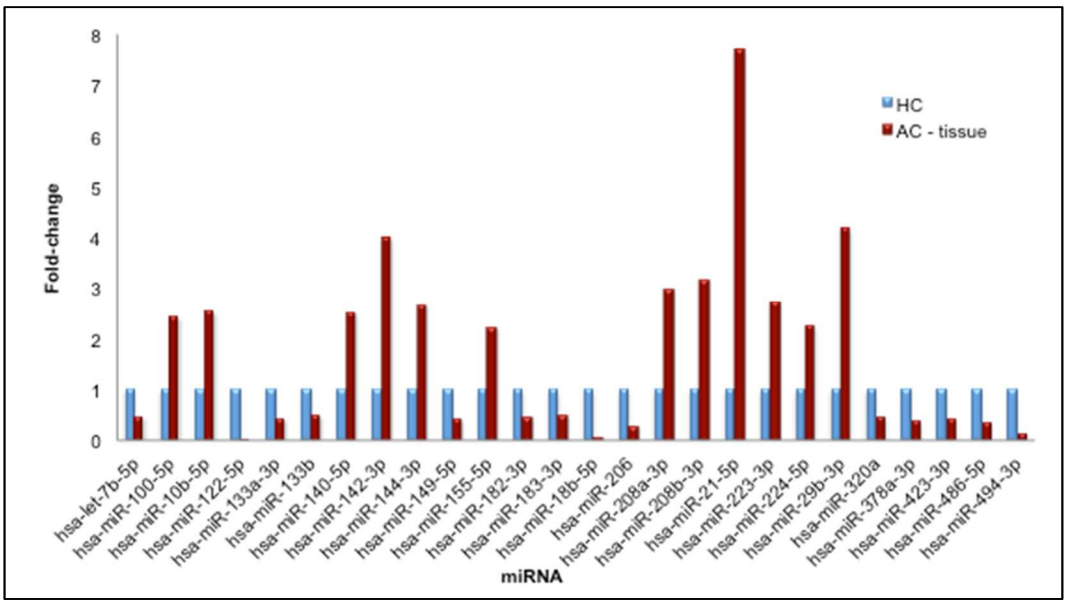

Figure 20: Representation of fold-change of differentially expressed miRNA in AC group (tissue samples) in comparison with HC.

Among them, 12 miRNAs presented a significant overexpressed fold-change greater than 2, and 14 showed a significant underexpressed fold-change lower than 0,5. Differentially expressed miRNA are listed in table 6.

miRNA differentially expressed in AC tissue samples vs HC.			
Number miRNAs upregulated		Number miRNAs downregulated	
12		14	
Fold-change miRNAs upregulated		Fold-change miRNAs downregulated	
hsa-miR-100-5p	2,45	**hsa-let-7b-5p**	0,49
hsa-miR-10b-5p	2,54	**hsa-miR-122-5p**	0,03
hsa-miR-140-5p	2,54	**hsa-miR-133a-3p**	0,44
hsa-miR-142-3p	4,02	**hsa-miR-133b**	0,49
hsa-miR-144-3p	2,69	**hsa-miR-149-5p**	0,42
hsa-miR-155-5p	2,24	**hsa-miR-18b-5p**	0,08
hsa-miR-208a-3p	3,00	**hsa-miR-182-3p**	0,47
hsa-miR-208b-3p	3,18	**Hsa-miR-183-3p**	0,50
hsa-miR-21-5p	7,73	**hsa-miR-206**	0,29
hsa-miR-223-3p	2,73	**hsa-miR-320a**	0,48
hsa-miR-224-5p	2,28	**hsa-miR-378a-3p**	0,39
hsa-miR-29b-3p	4,20	**hsa-miR-423-3p**	0,45
		hsa-miR-486-5p	0,37
		hsa-miR-494-3p	0,14

Table 6: Differentially expressed miRNA on AC group in comparison with HC from the analysis of tissue samples. It is specified the number of miRNAs, the list of over and under-expressed miRNAs and their fold-change values.

4.6.3 In silico analysis.

In silico analysis was performed on identified miRNA profiles, both on separately genotype-related profiles and on the unique AC profile. Prediction algorithms showed that PKP2/DSP and DSG2 profiles targeted genes involved in Hippo Signaling Pathway. Among differentially expressed miRNAs of PKP2/DSP profile, 12 miRNAs targeted a total of 92 Hippo-related genes (p-value 2,9e-9), such as NF2, TEAD1 (TEA domain transcription factor 1), LATS1, YAP1. On the other hand, 11 of the 14 differentially expressed miRNAs from DSG2 profile targeted 79 genes involved in Hippo Signaling Pathway (p-value 6,4e-6). Despite the identification of two different genotype-related profiles, *in silico* analysis demonstrated that both targeted genes involved in the same signaling pathway, which it has been previously correlated with AC pathogenesis (Chen et al., 2014).

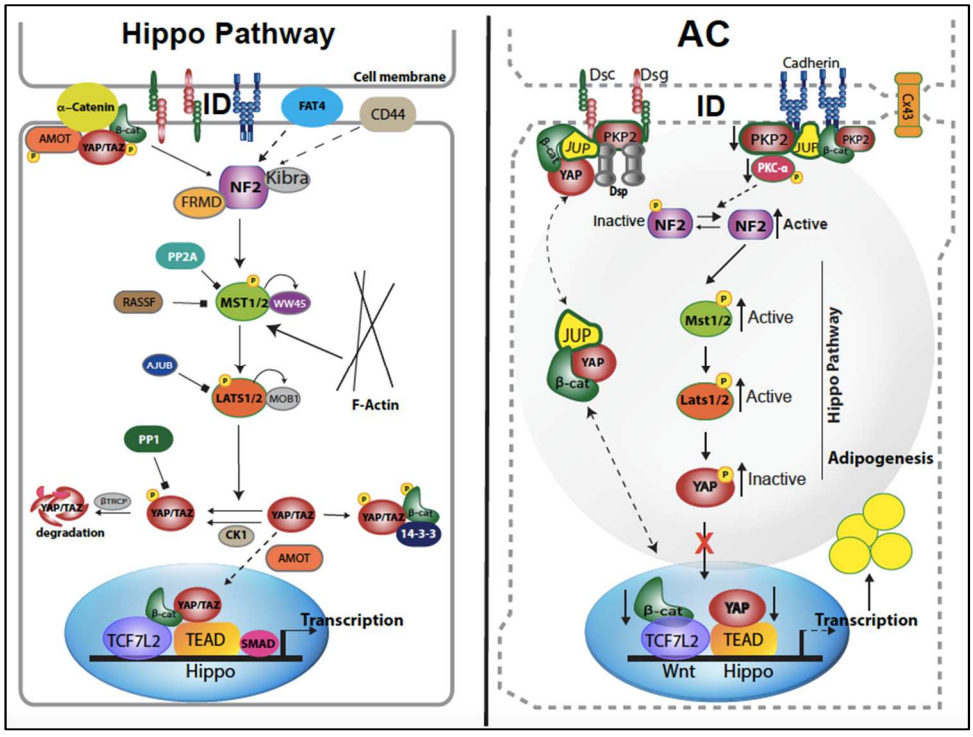

Figure 21: Schematic representation of Hippo signaling pathway. On the right, normal cascade and function of active Hippo pathway, on the left, impaired function with Hippo pathway inactivation in AC (from Chen et al. 2014).

In silico prediction algorithm on AC profile demonstrated that 20 of the 26 differentially expressed miRNAs targeted components involved in Arrhythmogenic Cardiomyopathy Pathway, such as JUP, DSG2 or DSP (p-value 0,03).

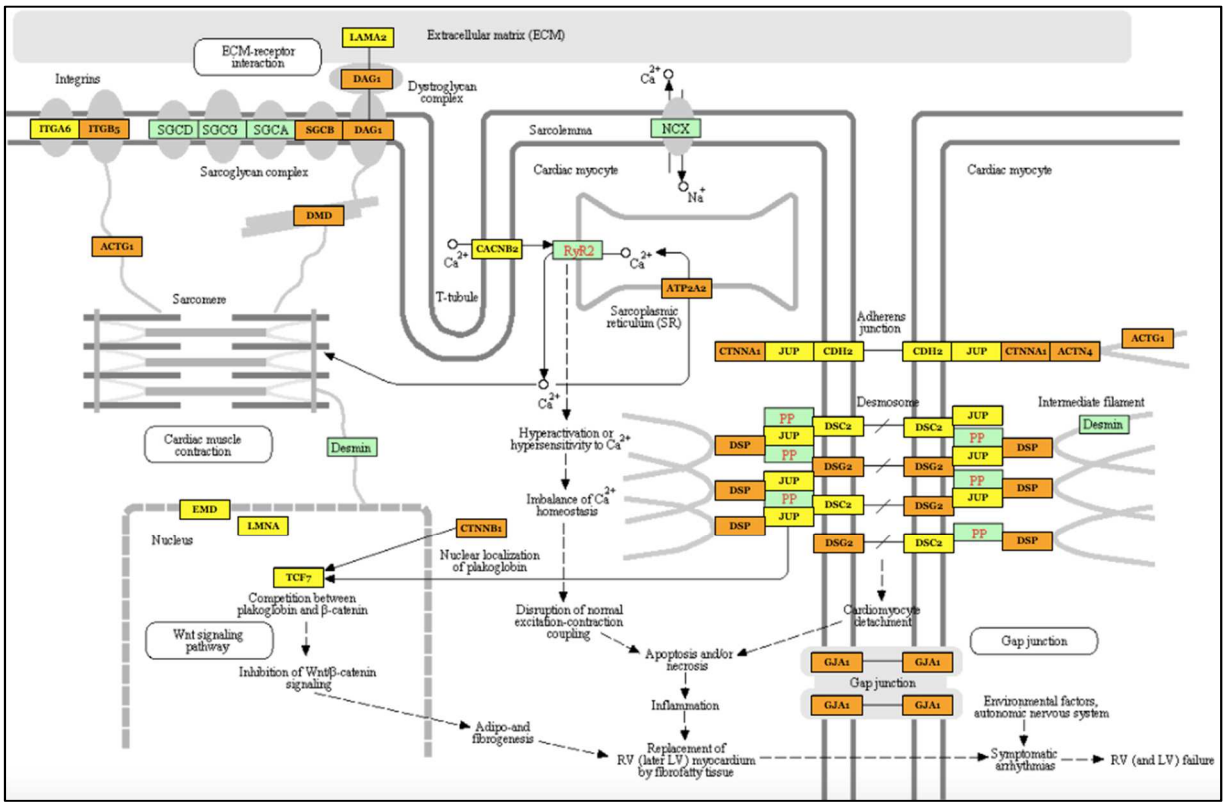

Figure 22: Schematic representation of AC Pathway. On orange and yellow, genes targeted by differentially expressed miRNAs from AC profile (from DIANA mirPath v.3).

4.7 miRNA expression profile analysis: blood samples.

84-miRNA array profiling was also performed in 9 whole blood samples from AC affected patients (5 PKP2, 2 DSP and 2 DSG2) and 4 HC showing a different miRNA expression profile comprising 14 miRNAs differentially expressed with respect to HC (Figure 23).

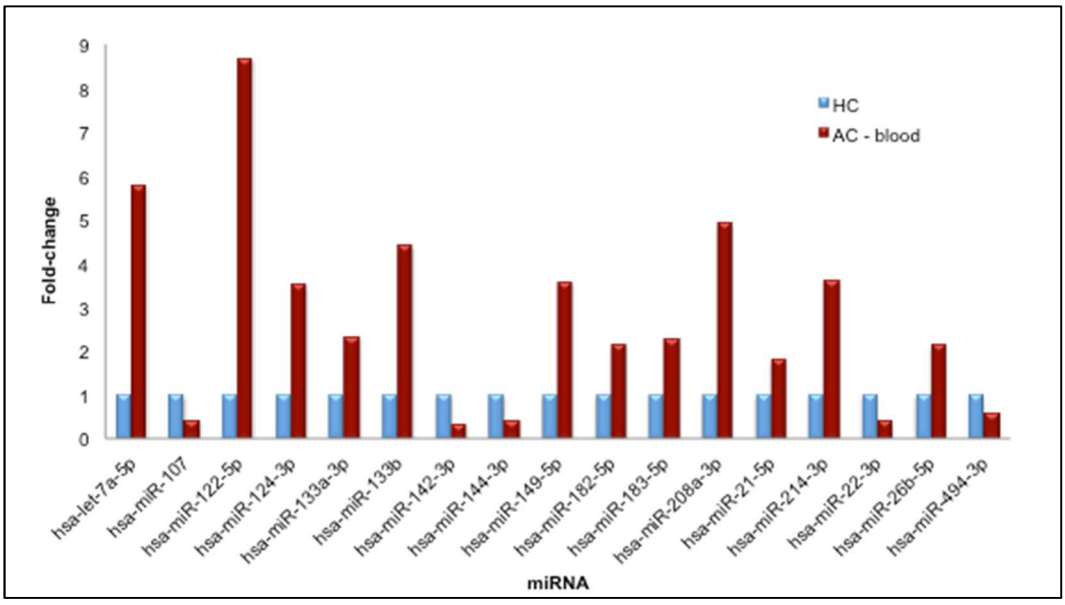

Figure 23: Representation of fold-change of differentially expressed miRNA in AC group (blood samples) in comparison with HC.

Among differentially expressed miRNAs, 10 presented a fold-change greater than 2, considered overexpressed; instead, 4 showed a fold-change lower than 0,5, considered underexpressed. The specific miRNAs over and underexpressed are listed in table 7.

miRNA differentially expressed in AC blood samples vs HC			
Number miRNAs upregulated		Number miRNAs downregulated	
10		4	
Fold-change miRNAs upregulated		**Fold-change miRNAs downregulated**	
hsa-let7a-5p	5,81	**hsa-miR-107**	0,43
hsa-miR-122-5p	8,69	**hsa-miR-142-3p**	0,35
hsa-miR-124-3p	3,54	**hsa-miR-144-3p**	0,43
hsa-miR-133a-3p	2,31	**hsa-miR-22-3p**	0,40
hsa-miR-133b	4,43		
hsa-miR-149-5p	3,60		
hsa-miR-182-5p	2,15		
hsa-miR-183-5p	2,29		
hsa-miR-214-3p	3,64		
hsa-miR-26b-5p	2,15		

Table 7: Differentially expressed miRNA on AC group in comparison with HC from the analysis of blood samples. It is specified the number of miRNAs, the list of over and under-expressed miRNAs and their fold-change values.

4.8 miRNA expression profile analysis: AC-tissue vs AC-blood samples.

Comparing miRNA expression profile identified in AC-group analysis from tissue and blood samples, 10 miRNAs were observed as differentially expressed in common in both analysis: hsa-miR-122-5p; hsa-miR-142-3p; hsa-miR-144-3p; hsa-miR-133a-3p; hsa-miR-133b; hsa-miR-149-5p; hsa-miR-182-3p; hsa-miR-183-3p; hsa-miR-494-3p (Figure 24).

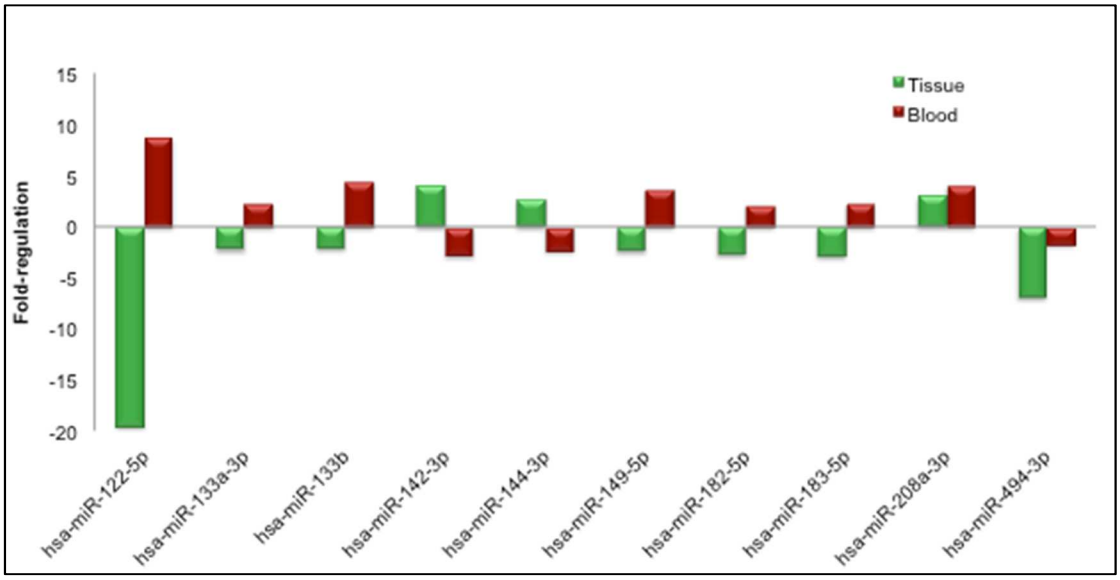

Figure 24: Representation of fold-regulation of the 10 miRNAs differentially expressed in both tissue and blood samples. In red, fold-regulation of blood samples; in green, of tissue samples.

Interestingly, most of them were inversely expressed in blood in comparison with tissue (Table 8). We identified 6 miRNAs that presented an overexpression in AC blood samples and an underexpression in AC tissue samples (hsa-miR-122-5p, hsa-miR-133a-3p, hsa-miR-133b, hsa-miR-149-5p, hsa-miR-182-3p, hsa-miR-183-3p). On the other hand, two miRNAs were also inversely expressed, but presented an underexpression in blood and overexpression in tissue (hsa-miR-142-3p and hsa-miR-144-3p). Instead, hsa-miR-208a-3p and hsa-miR-494-3p were identically expressed in tissue and blood samples, overexpressed and underexpressed respectively.

miRNA differentially expressed: AC-tissue vs AC-blood		
	Fold-regulation	
	AC-Tissue	AC-Blood
hsa-miR-122-5p	-19,56	8,70
hsa-miR-133a-3p	-2,26	2,32
hsa-miR-133b	-2,10	4,43
hsa-miR-142-3p	4,02	-2,84
hsa-miR-144-3p	2,69	-2,33
hsa-miR-149-5p	-2,38	3,60
hsa-miR-182-3p	-2,70	2,15
hsa-miR-183-5p	-2,88	2,28
hsa-miR-208a-3p	3,10	4,04
hsa-miR-494-3p	-7,01	-2

Table 8: Fold-regulation values of miRNA differentially expressed on AC-tissue and AC-blood samples.

4.9 Differentially expressed miRNA: validation

Among the 10 differentially expressed miRNAs identified in common on AC-tissue and AC-blood profiles, 4 miRNAs (hsa-miR-122-5p, hsa-miR-144-5p, hsa-miR-208a-3p and hsa-miR-494-3p) were validated in a larger cohort of 42 patients with a definite AC diagnosis and 8 HC. We additionally validated 3 miRNAs previously reported in the literature as implicated in fibrosis and AC: hsa-miR-21-5p (Thum et al., 2008, Zhang et al., 2016); hsa-miR-155-5p (Seok et al., 2014, Wei et al., 2017); hsa-miR-320a (Sommariva et al., 2017). In our miRNA profiling analysis in AC tissue samples; hsa-miR-21-5p and hsa-miR-155-5p were overexpressed with a fold-change of 7,73 and 2,24, respectively; instead, hsa-miR-320a resulted underexpressed with a fold-change of 0,4. However, they were not present in the AC-blood profile.

None of these miRNAs (hsa-miR-144-5p, hsa-miR-208a-3p, hsa-miR-494-3p, hsa-miR-21-5p, hsa-miR-155-5p and hsa-miR-320a) were confirmed in the larger 42-AC cohort as significantly differentially expressed in comparison with HC, since fold-change was around 1 (Table 9). Exception made for hsa-miR-122-5p which presented a 2,40-fold

change in AC patients comparing to HC, confirming that hsa-miR-122-5p was significantly overexpressed also in our larger cohort of AC blood samples comparing to HC.

Fold-change miRNA on 42 AC-blood samples	
hsa-miR-21-5p	0,83
hsa-miR-122-5p	2,40
hsa-miR-144-3p	1,14
hsa-miR-155-5p	1,10
hsa-miR-208a-3p	1,03
hsa-miR-494-3p	1,3
hsa-miR-320a	0,8

Table 9: Fold-change values of validated miRNA in 42 AC cohort in comparison with HC.

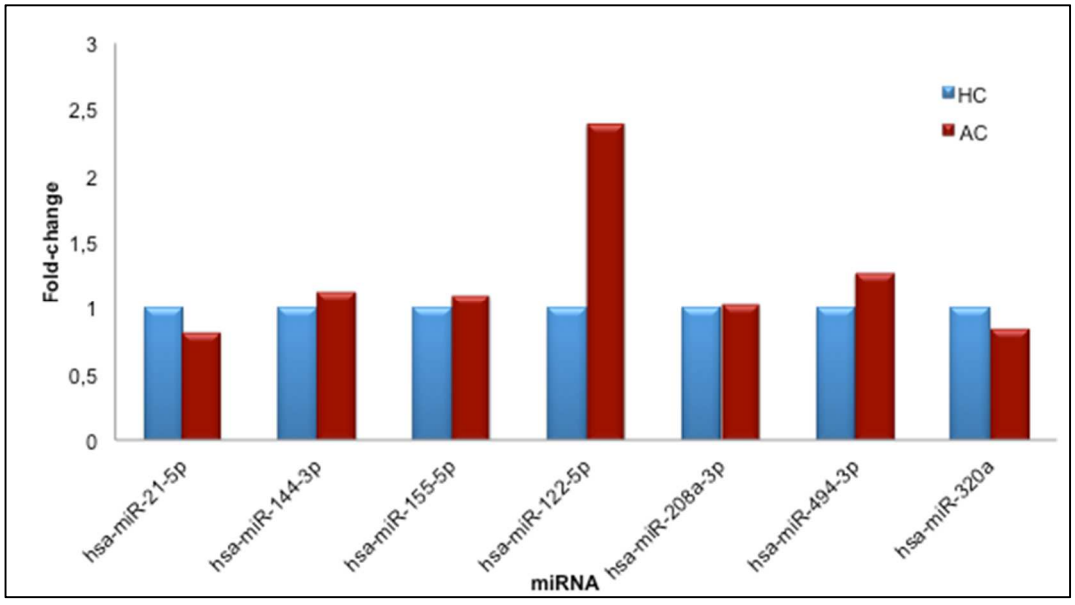

Figure 25: Representation of fold-change values of miRNA validated in 42 AC cohort in comparison with HC.

4.10 ROC curve analysis

We subsequently analysed fold-change values obtained from miRNA validation study by ROC curve analysis in order to determine if miRNAs may discriminate AC subjects from HC subjects. This analysis was performed loading fold-change values of every

miRNA of the validation study for each 50 samples (42 AC-subjects and 8 healthy controls) on MedCalc software. As represented on Figure 26, hsa-miR-21-5p, hsa-miR-144-5p, hsa-miR-155-5p, hsa-miR-208a-3p, hsa-miR-494-3p and hsa-miR320a presented AUC values near 0,5 (0,52 and 0,67), meaning their over or under-expression is not specific for the disease and is not able to distinguish AC from HC. Instead, hsa-miR-122-5p had an optimal AUC value of 0,83, giving evidence that this miRNA may be a potential prognostic biomarker which can distinguish AC subjects going in HF from HC, with a p-value<0,0001.

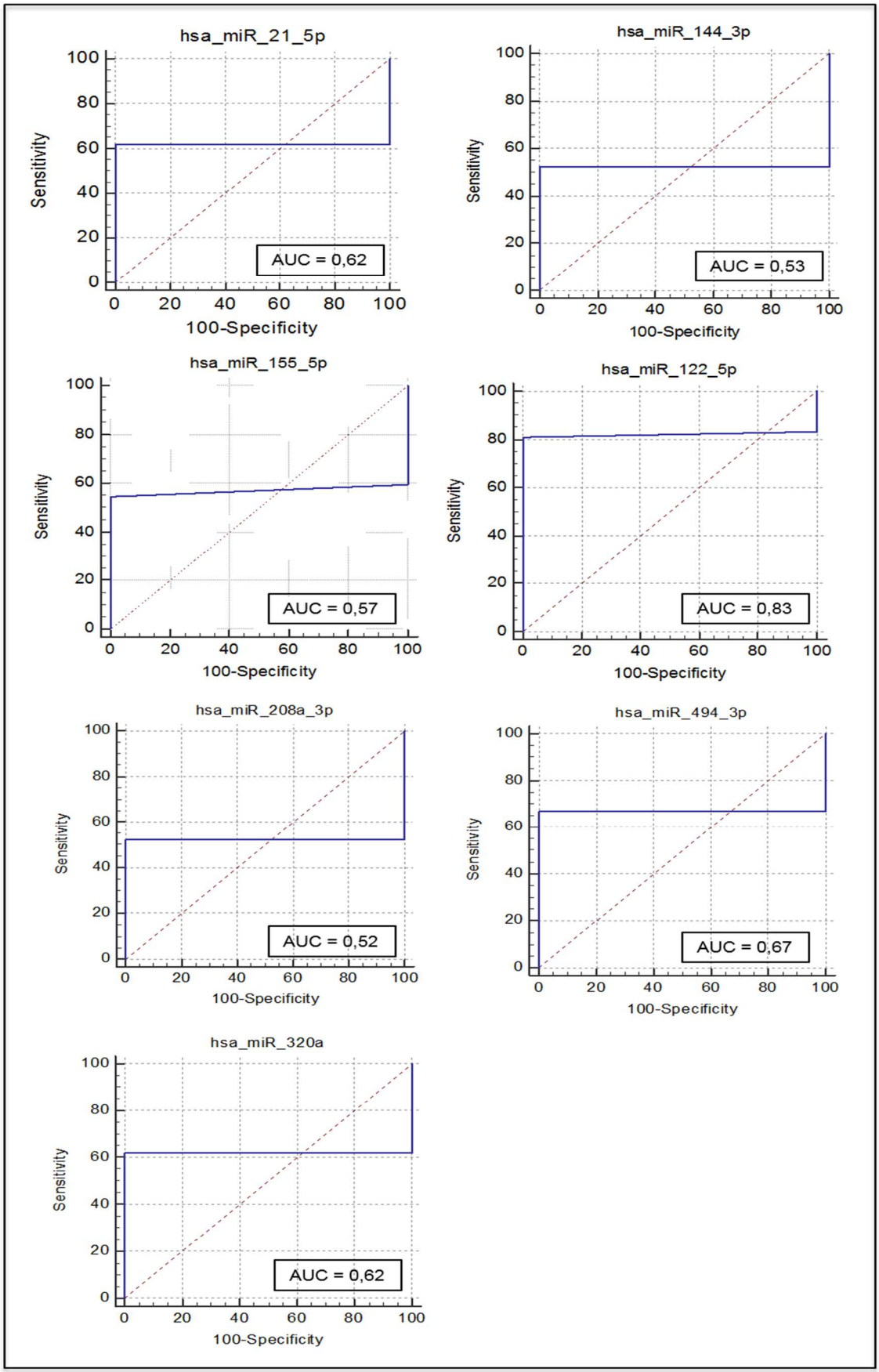

Figure 26: ROC curve and AUC values of validate miRNAs.

5 DISCUSSION

MicroRNAs are a group of endogenous short noncoding RNAs that regulate gene expression by sequence-specific recognition of their target transcripts (Bartel 2004). They are implicated in different cellular processes such as apoptosis, proliferation or differentiation. Aberrant levels of miRNAs have been reported as implicated in numerous pathophysiological conditions, including cardiovascular diseases and different type of cancers. Over or under-expression of determined miRNAs play a crucial role in tumour initiation, progression and metastasis (Yu et al., 2011). miRNA expression profiles have also been studied in “primary” cardiomyopathies such as HCM, DCM or AC; demonstrating that different cardiomyopathies may present a specific miRNA signature.

Arrhythmogenic Cardiomyopathy is a heart muscle disease clinically characterized by ventricular arrhythmias and high risk of sudden cardiac death, and pathologically by an acquired and progressive dystrophy of the ventricular myocardium with fibro-fatty replacement (Basso et al., 1996, Thiene et al., 1988) It is a genetically determined cardiomyopathy caused by heterozygous mutations in genes mostly encoding for proteins of the desmosomal complex, identified nearly on 50% of subjects and with low and age-dependent penetrance (Pilichou et al., 2016). Major and minor criteria were established and revised by an international Task Force for AC diagnosis (Marcus et al., 2010). Criteria consider cardiac morphology and function, tissue characterization, electric rhythm conduction and family history, including the identification of pathogenic mutations as major diagnostic criteria.

Thus, how the genetic, epigenetic and environmental factors synergy acts to modify disease phenotype and onset is crucial for understanding the pathophysiology of the disease (Basso et al., 2012a).

5.1 Meta-analysis: miRNAs in cardiomyopathies.

A meta-analysis of miRNA profiling in HCM, DCM and AC studies was carried out in order to determine whether miRNAs had been previously implicated in cardiomyopathies. We could observe how HCM was the most studied cardiomyopathy with numerous miRNAs associated with the disease. Instead, at the beginning of our experiments there was no study published about miRNAs in AC and its involvement in the disease. Up to now, three papers have been published describing: a miRNA profile in tissue samples of AC affected patients (Zhang et al., 2016), a miRNA profile in plasma samples of AC patients, identifying hsa-miR-320a as potential biomarker (Sommariva et al., 2017) and a miRNA profile in definite AC patients, identifying hsa-miR-494 as significantly overexpressed in definite AC patients with recurrent VA (Yamada et al., 2017). A fourth study demonstrated a downregulation of miR-184 in PKP2-deficient cells and AC models, associating the dysregulation of this miRNA with adipogenesis enhance (Gurha et al., 2016).

5.2 miRNA isolation.

RNA concentration obtained from tissue samples was higher (6 µg) compared to blood samples (600 ng). This is in keeping with the fact that there are low circulating miRNAs in blood samples than inside cells (Pritchard et al., 2012).

SNORD68 detection in all samples demonstrated the presence of small RNAs in extracts. In addition, miRTC was also revealed in order to determine the presence of inhibitors of reverse transcription and qPCR. Both assays resulted adequate as quality controls in order to select proper samples to go through downstream experiments, and as a consequence, reliable results.

5.3 miRNA expression profile in RV myocardial tissue from Arrhythmogenic Cardiomyopathy patients.

Eighty-four miRNAs screening was performed on 10 myocardial tissue samples (8 from AC affected subjects and 2 HC) and was identified a specific miRNA profile expression in AC patients. More specifically, a genotype-related signature was observed with PKP2 carriers presenting 19 differentially expressed miRNAs, DSP carriers 15 differentially expressed miRNAs and DSG2 carriers 14 miRNAs.

Comparing these genotype-related profiles, we observed an identical signature between PKP2 and DSP groups, with 14 dysregulated miRNAs in common, different from the 14 miRNAs found differentially expressed on DSG2 group. These findings indicated not only that there is a genotype-related miRNA profile but also that both, PKP2 and DSP carriers, presented a unique miRNA signature different from DSG2 carriers.

Despite the identification of two different miRNA expression profiles, *in silico* analysis demonstrated that both targeted the same signaling pathway, the Hippo signaling Pathway. In the PKP2/DSP profile, 12 dysregulated miRNAs targeted 92 Hippo-related genes (p-value 2,9e-9) whereas in the DSG2 profile 11 miRNAs targeted 79 genes involved in the same pathway (p-value 6,4e-6).

Activation of the Hippo signaling pathway is involved in AC (Chen et al., 2014) due to molecular changes at the IDs in patients with AC. Because of the impairment assembly of IDs, not only it is affected the mechanical integrity of myocyte-myocyte attachment but also the signaling events that are regulated at the IDs. On AC, NF2 is found to be activated, and as a consequence, a cascade of phosphorylation events takes place, including MST1/2, LATS1/2 and YAP (inactivated when phosphorylated). Consequently, gene expression through YAP-TEAD is suppressed. In addition, β-catenin is sequestered inactivating the canonical Wnt/β-catenin pathway. These molecular changes were associated with enhancing adipogenesis, as shifting the cell

fate toward an adipogenic lineage and the inactivation of YAP is implicated in protein kinase A (PKA) -induced adipogenesis. Furthermore, Hippo pathway regulates cardiac myocyte size and proliferation, postulating that its activation may be responsible of myocyte atrophy (Chen et al., 2014).

Our data, in keeping with this theory, demonstrated that hsa-miR-320a and hsa-miR-122-5p (PKP2/DSP profile) and also hsa-miR-155-5p and hsa-miR-224-5p (DSG2 profile) target LATS1/2 kinases. Further, hsa-miR-21-5p, overexpressed in PKP2/DSP profile, regulates NF2 and YAP. Both hsa-miR-122-5p and hsa-miR-155-5p target TEAD and show an underexpression in PKP2/DSP and DSG2 profiles respectively. The mechanism by which miRNAs differentially expressed are implicated in disease pathogenesis need further studies; however, we demonstrated that genotype-related profiles target genes of the Hippo signaling pathway, suggesting that there are many different roads to the regulation of the same pathway. This is in keeping with the fact that genes encode target sites for various miRNAs, so it is reasonable to assume that multiple miRNAs may act cooperatively to regulate important targets within a defined cellular or biological context (Grimson et al., 2007).

Subsequently analysis of all 8 myocardial tissue samples together as a unique AC group confirmed a common 26-miRNA signature including miRNAs differentially expressed in PKP2/DSP and DSG2 profiles. *In silico* analysis linked the implication of AC-profile to the AC pathway (p-value 0,03). The most significantly overexpressed miRNA was hsa-miR-21-5p (fold-change 7,73), which not only regulates genes implicated in Hippo signaling pathway but also interacts with DSP or DSC2, downregulating them (Pillai et al., 2014). Hsa-miR-21-5p overexpression may lead to a profoundly downregulation of these desmosomal components, causing a deeper impairment of the desmosome complex. On the other hand, hsa-miR-122-5p is the most underexpressed miRNA on AC-tissue profile (fold-change 0,03) and interacts with DSG2.

We proved that AC subjects showed a different and specific miRNA profile expression in comparison with HC. In addition, it is clear that miRNAs are implicated somehow in AC pathogenesis. Nevertheless, the specific mechanism of action and the correlation between differentially miRNA expression and desmosomal mutations need to be elucidated.

5.4 miRNA expression profile in whole blood from Arrhythmogenic Cardiomyopathy patients.

miRNA profiling was performed with the same 84-miRNA array on 13 whole blood samples, 9 from AC patients with a definite AC diagnosis and 4 HC. As previously reported, circulating miRNAs are extremely stable, often found in association with exosomes or proteins, and represent potentially informative biomarkers (Reid et al., 2011). Most of the studies performed miRNA identification on serum or plasma samples; on the contrary, we proved that miRNAs could be also detected on whole blood samples. As there is not a known housekeeping miRNA in order to normalize data, we used a spike-in control which is an exogenous miRNA that is added during miRNA isolation in order to normalize sample-to-sample reverse transcription and qPCR, thus leading to solid and reliable results.

We identified a different miRNA expression profile on AC patients in comparison with HC, where 14 miRNAs were differentially expressed (10 overexpressed and 4 underexpressed). However, grouping based on desmosomal mutations did not show a genotype-related expression profile of miRNAs in circulation. Although, we did show that circulating miRNAs in blood have a specific signature linked to AC.

5.5 miRNA expression profile in Arrhythmogenic Cardiomyopathy.

miRNA study on RV myocardial tissue samples of AC affected subjects demonstrated a specific miRNA signature in comparison with HC, corresponding to the differences in miRNA expression inside cells of the affected myocardium. Instead, in the blood study we demonstrated a characteristic miRNA profile, revealing differences in the expression of circulating miRNAs in AC patients, that might derive not only from affected cells but also from other blood components or other tissues. To distinguish miRNA expression from background miRNA noise we evaluated also blood samples from healthy controls and we substracted these data from our findings on AC patients.

Indeed, comparing miRNA profiles derived from tissue and blood AC samples 10 miRNAs were found differentially expressed in both myocardial tissue and in circulation. This evidence suggests that aberrant levels of miRNAs in circulation may reflect their differentially expression on myocardial tissue, as it was previously demonstrated for different types of cancer (Reid et al., 2011).

In particular, hsa-miR-122-5p, hsa-miR-133a-3p, hsa-miR-133b, hsa-miR-149-5p, hsa-miR-182-3p and hsa-miR-183-3p were inversely expressed, specifically in tissue these miRNAs were underexpressed and in blood overexpressed. On the contrary, hsa-miR-142-3p and hsa-miR-144-3p were overexpressed in tissue and underexpressed in circulation. Finally, hsa-miR-208a-3p and hsa-miR-494-3p were both over- and under-expressed in tissue and blood samples, respectively.

As reported in literature, miRNAs can be released from malignant, apoptotic or necrotic cells in circulation in different kind of tumours through vesicles. This transfer of material has been shown to contribute to tumour progression, modifications of the microenvironment and the host. The export of miRNAs from cells may be an important process for extracellular miRNA-signaling pathways, although this mechanism is not well understood (Cho et al., 2012, Palma et al., 2012, Webber et al., 2010).

Specific miRNA underexpression on tissue and overexpression in circulation make us hypothesize that miRNAs might be released in circulation from apoptotic or necrotic cardiomyocytes. Consequently, high levels of a specific miRNA may indicate disease progression, as its level increases when more cardiomyocytes go into cell death, releasing their content in circulation. These evidences suggest that overexpressed miRNAs in circulation may be potential prognostic biomarkers. On the contrary, miRNA overexpression in tissue might indicate cardiomyocyte malfunction.

5.6 miRNA validation: biomarkers identification.

Differentially expressed miRNAs identified in both, AC-blood and AC-tissue profiles were subsequently analysed in a larger cohort of 42 blood samples from AC affected subjects and 8 HC. AC subjects exhibited definite 2010 Task Force Criteria.

Additionally, 3 miRNAs were validated since they were identified differentially expressed in our AC-tissue profiling and previously reported as implicated in fibrosis and AC: hsa-miR-21-5p, hsa-miR-155-5p and hsa-miR-320a (Sommariva et al., 2017, Zhang et al., 2016).

5.6.1 Hsa-miR-144-3p

Hsa-miR-144-3p has been linked to different kind of cancers, such as gastric cancer, where it acts as tumour suppressor when overexpressed (Ren et al., 2017). In cardiovascular diseases, its role is not well understood but it has been associated to the prevention of cardiomyocyte death from ischemia-reperfusion (Slagsvold et al., 2014). Indeed. it has been also demonstrated that GATA-4-regulated miR-144/451 cluster confers cardiomyocyte-protective effect against simulated ischemia/reperfusion-induced cellular injury (Zhang et al., 2010). In addition, hsa-miR-144-3p plays a role in increasing the risk prediction in healthy individuals as part of the miRNA signature associated with future AMI (Bye et al., 2016). A recent study showed that plasma levels

of this miRNA were significantly elevated in definite AC patients with ventricular arrhythmias (VA) (Yamada et al., 2017).

Our data showed that hsa-miR-144-3p levels were high in AC-tissue profiling, while it presented an underexpression in our AC-blood profiling. Despite these findings, our validation data did not confirm dysregulation in 42-AC cohort compared to HC. ROC curve analysis could not distinguish AC from HC.

5.6.2 Hsa-miR-208a-3p

Hsa-miR-208a-3p is considered a “myomiR” as it is specifically expressed in cardiac tissue (Malizia and Wang 2011). The association with hsa-miR-370 was proposed as a promising biomarker for discriminating CAD (Liu et al., 2016). Therapeutic silencing of this miRNA attenuates myocyte apoptosis with subsequent improvement of cardiac function (Tony et al., 2015). Indeed, underexpression of hsa-miR-208a-3p, together with hsa-miR-208b-3p, hsa-miR-21-5p and hsa-miR-199a-5p in DCM patients under β-blockers predict the time-dependent reverse-remodelling response to therapy by decreasing apoptosis, cardiomyocyte cell death, hypertrophy and HF, and increasing contractile and overall cardiac functions (Sucharov et al., 2017). Further, hsa-miR-208a-3p has been associated with cardiac fibrosis by increasing endoglin expression to induce myocardial fibrosis in volume overloaded HF (Wang et al., 2014).

Our data showed hsa-miR-208a-3p significantly overexpressed in miRNA profiling on AC-blood samples and AC-tissue samples but its level in our 42-AC cohort was invariable (fold-change mean 1,03). ROC curve analysis confirmed that is not statistically different (AUC of 0.53).

5.6.3 Hsa-miR-494-3p

Hsa-miR-494-3p targets both pro-apoptotic and anti-apoptotic proteins, the ultimate consequence the Akt pathway activation, leading to cardioprotective effects against

ischemia/reperfusion injury (Wang et al., 2010). In addition, a recent study correlated this miRNA with AC by showing increased plasma levels of this miRNA in definite AC patients with the recurrence of VA after ablation (Yamada et al., 2017).

Levels of this miRNA in our 42-AC cohort were not significantly different between AC and HC; however, it presented an underexpression on both, AC-tissue and AC-blood profiling. Our validation study did not confirm these data and ROC curve analysis demonstrated no significant difference between AC and HC.

5.6.4 Hsa-miR-21-5p

Among the three miRNAs additionally validated on our large cohort, hsa-miR-21-5p has been already correlated as significantly overexpressed in heart tissues of AC patients (Zhang et al., 2016), on DCM patients (Rubiś et al., 2017) and associated with fibrosis on HCM patients (Fang et al., 2015). It has been shown that it regulates ERK-MAP kinase signaling pathway in cardiac fibroblast, which affects global cardiac structure and function. Its levels are increased selectively in fibroblasts of the failing heart, augmenting ERK-MAP kinase activity. This mechanism regulates fibroblast survival and growth factor secretion, apparently controlling the extent of interstitial fibrosis and cardiac hypertrophy (Thum et al., 2008). Further it has also been postulated as potential biomarker of RV failure, due to its increase during the phase of diastolic dysfunction indicating early RV fibrosis and its decline in plasma expression heralding the onset of systolic dysfunction (Reddy et al., 2017).

Our data confirmed a significant overexpression in myocardial tissue of AC patients, but AC-blood profiling did not validate this finding. Indeed, ROC curves display AUC equals to 0,62, supporting the fact that its expression was not significantly different between AC and HC in circulation.

5.6.5 Hsa-miR-155-5p

Hsa-miR-155-5p has been correlated to atherosclerosis, being specifically expressed in proinflammatory macrophages and promoting foam cell formation. This miRNA depletion in fibroblasts improved cardiac remodelling, one of the important causes of HF (Cao et al., 2016). Indeed, it has been reported that genetic loss of hsa-miR-155-5p ameliorates cardiac fibrotic remodelling following pressure overload. Therefore, inhibiting this miRNA may have potential as an adjunct to reduce cardiac inflammation in the treatment of cardiac fibrosis (Wei et al., 2017). In addition, inflammatory signaling through macrophage hsa-miR-155-5p modulated cardiac hypertrophy and failure during pressure overload (Heymans et al., 2013).

Our data showed that this miRNA is overexpressed in AC-tissue profiling, but it was not differentially expressed neither on AC-blood profiling nor in the validation study. ROC curve analysis demonstrated that levels of hsa-miR-155-5p on AC were not significantly different from levels on HC and is not able to distinguish both groups.

5.6.6 Hsa-miR-320a

Furthermore, a transcardiac gradient of miRNAs in HF has been identified showing hsa-miR-320a as overexpressed in the coronary sinus blood (Marques et al., 2016). Other authors supported that has-miR-320a together with hsa-miR-423-5p, hsa-miR-22 and hsa-miR-92b were used for the detection of HF patients in serum (Goren et al., 2012). In recent study, plasmatic hsa-miR-320a showed an underexpression in AC patients compared to controls (0,53-fold-change) and also to IVT; however, it was not correlated with AC severity (Sommariva et al., 2017).

Our findings showed that this miRNA was also underexpressed in our AC-tissue profiling, but no expression differences were found on our AC-blood profiling. Indeed, it did not present a significant differentially expression among our 42-AC cohort (0.8 fold-change) and ROC curve analysis demonstrated a low AUC value.

5.6.7 Hsa-miR-122-5p

Hsa-miR-122-5p was initially discovered as a liver-specific miRNA, but recently it was demonstrated to play important roles in various human diseases. Specifically, it has been reported the implication of hsa-miR-122-5p on AMI and its potentiality as prognostic biomarker. Levels of hsa-miR-122-5p were assessed in AMI patients and its overexpression was correlated with Troponin (classical marker for AMI). This evidence showed hsa-miR-122-5p as potential novel biomarker for AMI (Yao et al., 2015). In addition, a ratio between miR-122-5p/miR-133b has been identified as a new prognostic biomarker for the early identification of ST-segment elevation in AMI patients exhibiting a higher risk of developing major adverse events (Cortez-Dias et al., 2016). Furthermore, levels of circulating and in tissue miRNAs from failing hearts were analysed showing hsa-miR-122 to be released from the failing heart, suggesting its potential as biomarkers of HF (Marques et al., 2016).

In our study, hsa-miR-122-5p was significantly underexpressed in AC-tissue profile and interestingly, significantly overexpressed on AC-blood profile. Our validation cohort of 42 AC blood samples confirmed a 2,40 fold-change, considered significantly overexpressed. In addition, ROC curve of hsa-miR-122-5p demonstrated that this miRNA can significantly distinguish AC affected patients from HC, giving evidence of its potential as disease biomarker.

5.6.8 Potential AC biomarker.

miRNA-guided diagnostics is an increasingly powerful molecular approach for deriving clinically significant information from patient samples. To date, we know that miRNAs are excellent biomarkers due to their abundance, cell-type specificity and stability. Differential miRNA expression, not present only in myocardium but also in circulation, has the potential to be used as disease biomarker in clinical practise since miRNAs

analysis may be performed by non-invasive techniques; this makes endomyocardial biopsy not necessary to analyse tissue miRNA levels.

Among miRNAs analysed up to now only hsa-miR-122-5p can be potentially considered as AC biomarker. Underexpression of this miRNA in AC-tissue profile and subsequent validated overexpression in AC-blood samples make postulate a role of this miRNA in the prognosis of disease progression. Specifically, myocardial tissue samples derive from transplanted AC patients, considered in the end-stage phase of the disease, with HF. Instead, AC-blood profiling was analysed in variable stages of the disease but not as severe as that of AC-tissue samples profiling. Thus, we hypothesize that this miRNA may be released in the blood circulation from apoptotic or necrotic cardiomyocytes with increasing levels in the blood as disease progresses on myocardial tissue.

Whether hsa-miR-122-5p high levels indicate specific AC disease progression or represent a biomarker for HF in common with other cardiomyopathies need to be elucidated. Although, it can be a prognostic biomarker for disease progression toward HF. It is also necessary determine if released hsa-miR-122-5p may have a function into cell-to-cell communication or it is released during cell death. Nevertheless, we proved that hsa-miR-122-5p overexpression is meaningful on our 42-AC cohort giving strong evidence of its potentiality as AC diagnostic and prognostic biomarker.

6 REFERENCES

Ambros, V. *'microRNAs: tiny regulators with great potential'.* 2001., Cell, 107: 823-826

Ambros, V., Bartel, B., Bartel, D.P., Burge, C.B., Carrington, J.C., Chen, X., Dreyfuss, G., Eddy, S.R., Griffiths-Jones, S., Marshall, M., Matzke, M., Ruvkun, G., and Tuschl, T. *'A uniform system for microRNA annotation'.* 2003., RNA, 9: 277-279

Ameres, S.L., and Zamore, P.D. *'Diversifying microRNA sequence and function'.* 2013., Nat. Rev. Mol. Cell Biol., 14: 475-488

Asimaki, A., and Saffitz, J.E. *'Remodeling of cell-cell junctions in arrhythmogenic cardiomyopathy'.* 2014., Cell Commun. Adhes., 21: 13-23

Bartel, D.P. *'MicroRNAs: genomics, biogenesis, mechanism, and function'.* 2004., Cell, 116: 281

Basso, C., Thiene, G., Corrado, D., Angelini, A., Nava, A., and Valente, M. *'Arrhythmogenic right ventricular cardiomyopathy. Dysplasia, dystrophy, or myocarditis?'.* 1996., Circulation, 94: 983-991

Basso, C., Bauce, B., Corrado, D., and Thiene, G. *'Pathophysiology of arrhythmogenic cardiomyopathy'.* 2012a., Nature reviews. Cardiology, 9: 223-233

Basso, C., Corrado, D., Bauce, B., and Thiene, G. *'Arrhythmogenic right ventricular cardiomyopathy'.* 2012b., Circ Arrhythm Electrophysiol, 5: 1233-1246

Basso, C., Corrado, D., Marcus, F.I., Nava, A., and Thiene, G. *'Arrhythmogenic right ventricular cardiomyopathy'.* 2009., The Lancet, 373: 1289-1300

Bye, A., Røsjø, H., Nauman, J., Silva, G.J.J., Follestad, T., Omland, T., and Wisløff, U. *'Circulating microRNAs predict future fatal myocardial infarction in healthy individuals - The HUNT study'.* 2016., J. Mol. Cell. Cardiol., 97: 162-168

Calabrese, F., Basso, C., Carturan, E., Valente, M., and Thiene, G. *'Arrhythmogenic right ventricular cardiomyopathy/dysplasia: is there a role for viruses?'.* 2006., Cardiovasc. Pathol., 15: 11-17

Calin, G.A., Dumitru, C.D., Shimizu, M., Bichi, R., Zupo, S., Noch, E., Aldler, H., Rattan, S., Keating, M., Rai, K., Rassenti, L., Kipps, T., Negrini, M., Bullrich, F., and Croce, C.M. *'Frequent deletions and down-regulation of micro- RNA genes miR15 and miR16 at 13q14 in chronic lymphocytic leukemia'.* 2002., Proc. Natl. Acad. Sci. U.S.A., 99: 15524-15529

Cao, R.Y., Li, Q., Miao, Y., Zhang, Y., Yuan, W., Fan, L., Liu, G., Mi, Q., and Yang, J. *'The Emerging Role of MicroRNA-155 in Cardiovascular Diseases'.* 2016., Biomed Res Int, 2016: 9869208

Chen, S., Gurha, P., Lombardi, R., Ruggiero, A., Willerson, J., and Marian, A.J. *'The Hippo Pathway Is Activated and Is a Causal Mechanism for Adipogenesis in Arrhythmogenic Cardiomyopathy'.* 2014., Circulation Research, 114: 454-468

Cho, J.A., Park, H., Lim, E.H., and Lee, K.W. *'Exosomes from breast cancer cells can convert adipose tissue-derived mesenchymal stem cells into myofibroblast-like cells'.* 2012., Int. J. Oncol., 40: 130-138

Cho, K.W., Lee, J., and Kim, Y. *'Genetic Variations Leading to Familial Dilated Cardiomyopathy'.* 2016., Mol. Cells, 39: 722-727

Corrado, D., Basso, C., and Judge, D.P. *'Arrhythmogenic Cardiomyopathy'.* 2017., Circ. Res., 121: 784-802

Corsten, M.F., Dennert, R., Jochems, S., Kuznetsova, T., Devaux, Y., Hofstra, L., Wagner, D.R., Staessen, J.A., Heymans, S., and Schroen, B. *'Circulating MicroRNA-208b and MicroRNA-499 reflect myocardial damage in cardiovascular disease'.* 2010., Circ Cardiovasc Genet, 3: 499-506

Cortez-Dias, N., Costa, M.C., Carrilho-Ferreira, P., Silva, D., Jorge, C., Calisto, C., Pessoa, T., Robalo Martins, S., de Sousa, J.C., da Silva, P.C., Fiúza, M., Diogo, A.N., Pinto, F.J., and Enguita, F.J. *'Circulating miR-122-5p/miR-133b Ratio Is a Specific Early Prognostic Biomarker in Acute Myocardial Infarction'.* 2016., Circ. J., 80: 2183-2191

Creemers, E.E., Tijsen, A.J., and Pinto, Y.M. *'Circulating microRNAs: novel biomarkers and extracellular communicators in cardiovascular disease?'.* 2012., Circ. Res., 110: 483-495

d'Amati, G., di Gioia, C.R., Giordano, C., and Gallo, P. *'Myocyte transdifferentiation: a possible pathogenetic mechanism for arrhythmogenic right ventricular cardiomyopathy'.* 2000., Arch. Pathol. Lab. Med., 124: 287-290

Dellefave, L., and McNally, E.M. *'The genetics of dilated cardiomyopathy'.* 2010., Curr. Opin. Cardiol., 25: 198-204

Delmar, M., and McKenna, W.J. *'The cardiac desmosome and arrhythmogenic cardiomyopathies: from gene to disease'.* 2010., Circ. Res., 107: 700-714

DeLong, E.R., DeLong, D.M., and Clarke-Pearson, D.L. *'Comparing the areas under two or more correlated receiver operating characteristic curves: a nonparametric approach'.* 1988., Biometrics, 44: 837-845

Derda, A.A., Thum, S., Lorenzen, J.M., Bavendiek, U., Heineke, J., Keyser, B., Stuhrmann, M., Givens, R.C., Kennel, P.J., Schulze, P.C., Widder, J.D., Bauersachs, J., and Thum, T. *'Blood-based microRNA signatures differentiate various forms of cardiac hypertrophy'.* 2015., Int. J. Cardiol., 196: 115-122

Doench, J.G., Petersen, C.P., and Sharp, P.A. *'siRNAs can function as miRNAs'.* 2003., Genes Dev., 17: 438-442

Fang, L., Ellims, A.H., Moore, X., White, D.A., Taylor, A.J., Chin-Dusting, J., and Dart, A.M. *'Circulating microRNAs as biomarkers for diffuse myocardial fibrosis in patients with hypertrophic cardiomyopathy'.* 2015., J Transl Med, 13: 314

Fichtlscherer, S., De Rosa, S., Fox, H., Schwietz, T., Fischer, A., Liebetrau, C., Weber, M., Hamm, C.W., Röxe, T., Müller-Ardogan, M., Bonauer, A., Zeiher, A.M., and Dimmeler, S. *'Circulating microRNAs in patients with coronary artery disease'.* 2010., Circ. Res., 107: 677-684

Fiedler, J., and Thum, T. *'New Insights Into miR-17-92 Cluster Regulation and Angiogenesis'.* 2016., Circ. Res., 118: 9-11

Fire, A., Xu, S., Montgomery, M.K., Kostas, S.A., Driver, S.E., and Mello, C.C. *'Potent and specific genetic interference by double-stranded RNA in Caenorhabditis elegans'.* 1998., Nature, 391: 806-811

Franke, W.W., Borrmann, C.M., Grund, C., and Pieperhoff, S. *'The area composita of adhering junctions connecting heart muscle cells of vertebrates. I. Molecular definition in intercalated disks of cardiomyocytes by immunoelectron microscopy of desmosomal proteins'.* 2006., Eur. J. Cell Biol., 85: 69-82

Garcia-Gras, E., Lombardi, R., Giocondo, M.J., Willerson, J.T., Schneider, M.D., Khoury, D.S., and Marian, A.J. *'Suppression of canonical Wnt/beta-catenin signaling by nuclear plakoglobin recapitulates phenotype of arrhythmogenic right ventricular cardiomyopathy'.* 2006., J. Clin. Invest., 116: 2012-2021

Garrod, S., and Pickering, M.J. *'Joint action, interactive alignment, and dialog'.* 2009., Top Cogn Sci, 1: 292-304

Gerull, B., Heuser, A., Wichter, T., Paul, M., Basson, C.T., McDermott, D.A., Lerman, B.B., Markowitz, S.M., Ellinor, P.T., MacRae, C.A., Peters, S., Grossmann, K.S., Drenckhahn, J., Michely, B., Sasse-Klaassen, S., Birchmeier, W., Dietz, R., Breithardt, G., Schulze-Bahr, E., and Thierfelder, L. *'Mutations in the desmosomal protein plakophilin-2 are common in arrhythmogenic right ventricular cardiomyopathy'.* 2004., Nat. Genet., 36: 1162-1164

Goren, Y., Kushnir, M., Zafrir, B., Tabak, S., Lewis, B.S., and Amir, O. *'Serum levels of microRNAs in patients with heart failure'.* 2012., European Journal of Heart Failure, 14: 147-154

Grimson, A., Farh, K.K., Johnston, W.K., Garrett-Engele, P., Lim, L.P., and Bartel, D.P. *'MicroRNA targeting specificity in mammals: determinants beyond seed pairing'.* 2007., Mol. Cell, 27: 91-105

Gupta, P., Liu, B., Wu, J.Q., Soriano, V., Vispo, E., Carroll, A.P., Goldie, B.J., Cairns, M.J., and Saksena, N.K. *'Genome-wide mRNA and miRNA analysis of peripheral blood mononuclear cells (PBMC) reveals different miRNAs regulating HIV/HCV co-infection'.* 2014., Virology, 450-451: 336-349

Gurha, P., Chen, X., Lombardi, R., Willerson, J., and Marian, A. *'Knockdown of Plakophilin 2 Downregulates miR-184 Through CpG Hypermethylation and Suppression of the E2F1 Pathway and Leads to Enhanced Adipogenesis In Vitro'.* 2016., Circulation Research, 119: 731-750

Han, J., Lee, Y., Yeom, K., Nam, J., Heo, I., Rhee, J., Sohn, S.Y., Cho, Y., Zhang, B., and Kim, V.N. *'Molecular basis for the recognition of primary microRNAs by the Drosha-DGCR8 complex'.* 2006., Cell, 125: 887-901

Hannon, G.J. *'RNA interference'.* 2002., Nature, 418: 244-251

Heymans, S., Corsten, M.F., Verhesen, W., Carai, P., van Leeuwen, Rick E W, Custers, K., Peters, T., Hazebroek, M., Stöger, L., Wijnands, E., Janssen, B.J., Creemers, E.E., Pinto, Y.M., Grimm, D., Schürmann, N., Vigorito, E., Thum, T., Stassen, F., Yin, X., Mayr, M., de Windt, L.J., Lutgens, E., Wouters, K., de Winther, Menno P J, Zacchigna, S., Giacca, M., van Bilsen, M., Papageorgiou, A., and Schroen, B. *'Macrophage microRNA-155 promotes cardiac hypertrophy and failure'.* 2013., Circulation, 128: 1420-1432

Kleber, A.G., and Saffitz, J.E. *'Role of the intercalated disc in cardiac propagation and arrhythmogenesis'.* 2014., Front Physiol, 5: 404

Kozomara, A., and Griffiths-Jones, S. *'miRBase: annotating high confidence microRNAs using deep sequencing data'.* 2014., Nucleic Acids Res., 42: 68

Kuster, D.W.D., Mulders, J., Ten Cate, F.J., Michels, M., Dos Remedios, C.G., da Costa Martins, Paula A, van der Velden, J., and Oudejans, C.B.M. *'MicroRNA transcriptome profiling in cardiac tissue of hypertrophic cardiomyopathy patients with MYBPC3 mutations'.* 2013., J. Mol. Cell. Cardiol., 65: 59-66

Kuwabara, Y., Ono, K., Horie, T., Nishi, H., Nagao, K., Kinoshita, M., Watanabe, S., Baba, O., Kojima, Y., Shizuta, S., Imai, M., Tamura, T., Kita, T., and Kimura, T. *'Increased microRNA-1 and microRNA-133a levels in serum of patients with cardiovascular disease indicate myocardial damage'.* 2011., Circ Cardiovasc Genet, 4: 446-454

Lagos-Quintana, M., Rauhut, R., Lendeckel, W., and Tuschl, T. *'Identification of novel genes coding for small expressed RNAs'.* 2001., Science, 294: 853-858

Lai, E.C. *'Micro RNAs are complementary to 3' UTR sequence motifs that mediate negative post-transcriptional regulation'.* 2002., Nat. Genet., 30: 363-364

Landi, M.T., Zhao, Y., Rotunno, M., Koshiol, J., Liu, H., Bergen, A.W., Rubagotti, M., Goldstein, A.M., Linnoila, I., Marincola, F.M., Tucker, M.A., Bertazzi, P.A., Pesatori, A.C., Caporaso, N.E., McShane, L.M., and Wang, E. *'MicroRNA expression differentiates histology and predicts survival of lung cancer'.* 2010., Clin. Cancer Res., 16: 430-441

Latronico, M.V.G., and Condorelli, G. *'MicroRNAs and cardiac pathology'.* 2009., Nat Rev Cardiol, 6: 419-429

Latronico, M.V.G., and Condorelli, G. *'Therapeutic applications of noncoding RNAs'.* 2015., Curr. Opin. Cardiol., 30: 213-221

Lau, N.C., Lim, L.P., Weinstein, E.G., and Bartel, D.P. *'An abundant class of tiny RNAs with probable regulatory roles in Caenorhabditis elegans'.* 2001., Science, 294: 858-862

Lee, R.C., Feinbaum, R.L., and Ambros, V. *'The C. elegans heterochronic gene lin-4 encodes small RNAs with antisense complementarity to lin-14'.* 1993., Cell, 75: 843-854

Lee, Y., Ahn, C., Han, J., Choi, H., Kim, J., Yim, J., Lee, J., Provost, P., Rådmark, O., Kim, S., and Kim, V.N. *'The nuclear RNase III Drosha initiates microRNA processing'.* 2003., Nature, 425: 415-419

Liew, C., Ma, J., Tang, H., Zheng, R., and Dempsey, A.A. *'The peripheral blood transcriptome dynamically reflects system wide biology: a potential diagnostic tool'.* 2006., J. Lab. Clin. Med., 147: 126-132

Liu, H., Yang, N., Fei, Z., Qiu, J., Ma, D., Liu, X., Cai, G., and Li, S. *'Analysis of plasma miR-208a and miR-370 expression levels for early diagnosis of coronary artery disease'.* 2016., Biomed Rep, 5: 332-336

Lombardi, R., da Graca Cabreira-Hansen, M., Bell, A., Fromm, R.R., Willerson, J.T., and Marian, A.J. *'Nuclear plakoglobin is essential for differentiation of cardiac progenitor cells to adipocytes in arrhythmogenic right ventricular cardiomyopathy'.* 2011., Circ. Res., 109: 1342-1353

Malizia, A.P., and Wang, D. *'MicroRNAs in cardiomyocyte development'.* 2011., Wiley Interdiscip Rev Syst Biol Med, 3: 183-190

Marcus, F.I., McKenna, W.J., Sherrill, D., Basso, C., Bauce, B., Bluemke, D.A., Calkins, H., Corrado, D., Cox, Moniek G P J, Daubert, J.P., Fontaine, G., Gear, K., Hauer, R., Nava, A., Picard, M.H., Protonotarios, N., Saffitz, J.E., Sanborn, D.M.Y., Steinberg, J.S., Tandri, H., Thiene, G., Towbin, J.A., Tsatsopoulou, A., Wichter, T., and

Zareba, W. *'Diagnosis of arrhythmogenic right ventricular cardiomyopathy/dysplasia: proposed modification of the Task Force Criteria'.* 2010., Eur. Heart J., 31: 806-814

Maron, B.J., Haas, T.S., and Goodman, J.S. *'Hypertrophic cardiomyopathy: one gene … but many phenotypes'.* 2014., Am. J. Cardiol., 113: 1772-1773

Maron, B.J., Towbin, J.A., Thiene, G., Antzelevitch, C., Corrado, D., Arnett, D., Moss, A.J., Seidman, C.E., and Young, J.B. *'Contemporary Definitions and Classification of the Cardiomyopathies: An American Heart Association Scientific Statement From the Council on Clinical Cardiology, Heart Failure and Transplantation Committee; Quality of Care and Outcomes Research and Functional Genomics and Translational Biology Interdisciplinary Working Groups; and Council on Epidemiology and Prevention'.* 2006., Circulation, 113: 1807-1816

Marques, F.Z., Vizi, D., Khammy, O., Mariani, J.A., and Kaye, D.M. *'The transcardiac gradient of cardio-microRNAs in the failing heart'.* 2016., Eur. J. Heart Fail., 18: 1000-1008

McKenna, W.J., Thiene, G., Nava, A., Fontaliran, F., Blomstrom-Lundqvist, C., Fontaine, G., and Camerini, F. *'Diagnosis of arrhythmogenic right ventricular dysplasia/cardiomyopathy. Task Force of the Working Group Myocardial and Pericardial Disease of the European Society of Cardiology and of the Scientific Council on Cardiomyopathies of the International Society and Federation of Cardiology'.* 1994., Br Heart J, 71: 215-218

McKoy, G., Protonotarios, N., Crosby, A., Tsatsopoulou, A., Anastasakis, A., Coonar, A., Norman, M., Baboonian, C., Jeffery, S., and McKenna, W.J. *'Identification of a deletion in plakoglobin in arrhythmogenic right ventricular cardiomyopathy with palmoplantar keratoderma and woolly hair (Naxos disease)'.* 2000., Lancet, 355: 2119-2124

Meister, G., Landthaler, M., Patkaniowska, A., Dorsett, Y., Teng, G., and Tuschl, T. *'Human Argonaute2 mediates RNA cleavage targeted by miRNAs and siRNAs'.* 2004., Mol. Cell, 15: 185-197

Mencía, A., Modamio-Høybjør, S., Redshaw, N., Morín, M., Mayo-Merino, F., Olavarrieta, L., Aguirre, L.A., del Castillo, I., Steel, K.P., Dalmay, T., Moreno, F., and Moreno-Pelayo, M.A. *'Mutations in the seed region of human miR-96 are responsible for nonsyndromic progressive hearing loss'.* 2009., Nat. Genet., 41: 609-613

Norgett, E.E., Hatsell, S.J., Carvajal-Huerta, L., Cabezas, J.C., Common, J., Purkis, P.E., Whittock, N., Leigh, I.M., Stevens, H.P., and Kelsell, D.P. *'Recessive mutation in desmoplakin disrupts desmoplakin-intermediate filament interactions and causes dilated cardiomyopathy, woolly hair and keratoderma'.* 2000., Hum. Mol. Genet., 9: 2761-2766

North, A.J., Bardsley, W.G., Hyam, J., Bornslaeger, E.A., Cordingley, H.C., Trinnaman, B., Hatzfeld, M., Green, K.J., Magee, A.I., and Garrod, D.R. *'Molecular map of the desmosomal plaque'.* 1999., J. Cell. Sci., 112 (Pt 23): 4325-4336

Olena, A.F., and Patton, J.G. *'Genomic organization of microRNAs'.* 2010., J. Cell. Physiol., 222: 540-545

Palacín, M., Coto, E., Reguero, J.R., Morís, C., and Alvarez, V. *'Profile of microRNAs in the plasma of hypertrophic cardiomyopathy patients compared to healthy controls'.* 2013., Int. J. Cardiol., 167: 3075-3076

Palacín, M., Reguero, J.R., Martín, M., Díaz Molina, B., Morís, C., Alvarez, V., and Coto, E. *'Profile of microRNAs differentially produced in hearts from patients with hypertrophic cardiomyopathy and sarcomeric mutations'.* 2011., Clin. Chem., 57: 1614-1616

Palma, J., Yaddanapudi, S.C., Pigati, L., Havens, M.A., Jeong, S., Weiner, G.A., Weimer, K.M.E., Stern, B., Hastings, M.L., and Duelli, D.M. *'MicroRNAs are exported from malignant cells in customized particles'.* 2012., Nucleic Acids Res., 40: 9125-9138

Pasquinelli, A.E., Reinhart, B.J., Slack, F., Martindale, M.Q., Kuroda, M.I., Maller, B., Hayward, D.C., Ball, E.E., Degnan, B., Müller, P., Spring, J., Srinivasan, A., Fishman, M., Finnerty, J., Corbo, J., Levine, M., Leahy, P., Davidson, E., and Ruvkun, G. *'Conservation of the sequence and temporal expression of let-7 heterochronic regulatory RNA'.* 2000., Nature, 408: 86-89

Patel, D., Gemel, J., Xu, Q., Simon, A.R., Lin, X., Matiukas, A., Beyer, E.C., and Veenstra, R.D. *'Atrial fibrillation-associated connexin40 mutants make hemichannels and synergistically form gap junction channels with novel properties'.* 2014., FEBS Lett., 588: 1458-1464

Pilichou, K., Lazzarini, E., Rigato, I., Celeghin, R., De Bortoli, M., Perazzolo Marra, M., Cason, M., Jongbloed, J., Calore, M., Rizzo, S., Regazzo, D., Poloni, G., Iliceto, S., Daliento, L., Delise, P., Corrado, D., Van Tintelen, J.P., Thiene, G., Rampazzo, A., Basso, C., Bauce, B., Lorenzon, A., and Occhi, G. *'Large Genomic Rearrangements of Desmosomal Genes in Italian Arrhythmogenic Cardiomyopathy Patients'.* 2017., Circ Arrhythm Electrophysiol, 10

Pilichou, K., Nava, A., Basso, C., Beffagna, G., Bauce, B., Lorenzon, A., Frigo, G., Vettori, A., Valente, M., Towbin, J., Thiene, G., Danieli, G.A., and Rampazzo, A. *'Mutations in desmoglein-2 gene are associated with arrhythmogenic right ventricular cardiomyopathy'.* 2006., Circulation, 113: 1171-1179

Pilichou, K., Remme, C.A., Basso, C., Campian, M.E., Rizzo, S., Barnett, P., Scicluna, B.P., Bauce, B., van den Hoff, Maurice J B, de Bakker, Jacques M T, Tan, H.L., Valente, M., Nava, A., Wilde, A.A.M., Moorman, A.F.M., Thiene, G., and Bezzina, C.R. *'Myocyte necrosis underlies progressive myocardial dystrophy in mouse dsg2-related arrhythmogenic right ventricular cardiomyopathy'.* 2009., J. Exp. Med., 206: 1787-1802

Pilichou, K., Thiene, G., Bauce, B., Rigato, I., Lazzarini, E., Migliore, F., Perazzolo Marra, M., Rizzo, S., Zorzi, A., Daliento, L., Corrado, D., and Basso, C. *'Arrhythmogenic cardiomyopathy'.* 2016., Orphanet J Rare Dis, 11: 33

Pillai, M.M., Gillen, A.E., Yamamoto, T.M., Kline, E., Brown, J., Flory, K., Hesselberth, J.R., and Kabos, P. *'HITS-CLIP reveals key regulators of nuclear receptor signaling in breast cancer'.* 2014., Breast Cancer Res. Treat., 146: 85-97

Pritchard, C.C., Cheng, H.H., and Tewari, M. *'MicroRNA profiling: approaches and considerations'.* 2012., Nature reviews. Genetics, 13: 358

Reddy, S., Hu, D., Zhao, M., Blay, E., Sandeep, N., Ong, S., Jung, G., Kooiker, K.B., Coronado, M., Fajardo, G., and Bernstein, D. *'miR-21 is associated with fibrosis and right ventricular failure'.* 2017., JCI Insight, 2

Reid, G., Kirschner, M.B., and van Zandwijk, N. *'Circulating microRNAs: Association with disease and potential use as biomarkers'.* 2011., Critical Reviews in Oncology / Hematology, 80: 193-208

Reinhart, B.J., Slack, F.J., Basson, M., Pasquinelli, A.E., Bettinger, J.C., Rougvie, A.E., Horvitz, H.R., and Ruvkun, G. *'The 21-nucleotide let-7 RNA regulates developmental timing in Caenorhabditis elegans'.* 2000., Nature, 403: 901-906

Ren, K., Liu, Q.-., An, Z.-., Zhang, D.-., and Chen, X.-. *'MiR-144 functions as tumor suppressor by targeting PIM1 in gastric cancer'.* 2017., Eur Rev Med Pharmacol Sci, 21: 3028-3037

Rodriguez, A., Griffiths-Jones, S., Ashurst, J.L., and Bradley, A. *'Identification of mammalian microRNA host genes and transcription units'.* 2004., Genome Res., 14: 1902-1910

Roma-Rodrigues, C., Raposo, L.R., and Fernandes, A.R. *'MicroRNAs Based Therapy of Hypertrophic Cardiomyopathy: The Road Traveled So Far'.* 2015., BioMed research international, 2015: 983290

Roncarati, R., Viviani Anselmi, C., Losi, M.A., Papa, L., Cavarretta, E., Da Costa Martins, P., Contaldi, C., Saccani Jotti, G., Franzone, A., Galastri, L., Latronico, M.V.G., Imbriaco, M., Esposito, G., De Windt, L., Betocchi, S., and Condorelli, G. *'Circulating miR-29a, among other up-regulated microRNAs, is the only biomarker for both hypertrophy and fibrosis in patients with hypertrophic cardiomyopathy'.* 2014., J. Am. Coll. Cardiol., 63: 920-927

Rubiś, P., Totoń-Żurańska, J., Wiśniowska-Śmiałek, S., Holcman, K., Kołton-Wróż, M., Wołkow, P., Wypasek, E., Natorska, J., Rudnicka-Sosin, L., Pawlak, A., Kozanecki, A., and Podolec, P. *'Relations between circulating microRNAs (miR-21, miR-26, miR-29, miR-30 and miR-133a), extracellular matrix fibrosis and serum markers of fibrosis in dilated cardiomyopathy'.* 2017., Int. J. Cardiol., 231: 201-206

Schwarz, D.S., Hutvágner, G., Du, T., Xu, Z., Aronin, N., and Zamore, P.D. *'Asymmetry in the assembly of the RNAi enzyme complex'.* 2003., Cell, 115: 199-208

Schwarzenbach, H., Nishida, N., Calin, G.A., and Pantel, K. *'Clinical relevance of circulating cell-free microRNAs in cancer'.* 2014., Nat Rev Clin Oncol, 11: 145-156

Seok, H., Chen, J., Kataoka, M., Huang, Z., Ding, J., Yan, J., Hu, X., and Wang, D. *'Loss of MicroRNA-155 Protects the Heart From Pathological Cardiac Hypertrophy'.* 2014., Circulation Research, 114: 1585-1595

Slagsvold, K.H., Johnsen, A.B., Rognmo, O., Høydal, M.A., Wisløff, U., and Wahba, A. *'Mitochondrial respiration and microRNA expression in right and left atrium of patients with atrial fibrillation'.* 2014., Physiol. Genomics, 46: 505-511

Sommariva, E., D'Alessandra, Y., Farina, F.M., Casella, M., Cattaneo, F., Catto, V., Chiesa, M., Stadiotti, I., Brambilla, S., Dello Russo, A., Carbucicchio, C., Vettor, G., Riggio, D., Sandri, M.T., Barbuti, A., Vernillo, G., Muratori, M., Dal Ferro, M., Sinagra, G., Moimas, S., Giacca, M., Colombo, G.I., Pompilio, G., and Tondo, C. *'MiR-320a as a Potential Novel Circulating Biomarker of Arrhythmogenic CardioMyopathy'.* 2017., Sci Rep, 7: 4802

Spirito, P., Autore, C., Formisano, F., Assenza, G.E., Biagini, E., Haas, T.S., Bongioanni, S., Semsarian, C., Devoto, E., Musumeci, B., Lai, F., Yeates, L., Conte, M.R., Rapezzi, C., Boni, L., and Maron, B.J. *'Risk of sudden death and outcome in patients with hypertrophic cardiomyopathy with benign presentation and without risk factors'.* 2014., Am. J. Cardiol., 113: 1550-1555

Sucharov, C.C., Kao, D.P., Port, J.D., Karimpour-Fard, A., Quaife, R.A., Minobe, W., Nunley, K., Lowes, B.D., Gilbert, E.M., and Bristow, M.R. *'Myocardial microRNAs associated with reverse remodeling in human heart failure'.* 2017., JCI Insight, 2: e89169

Syrris, P., Ward, D., Evans, A., Asimaki, A., Gandjbakhch, E., Sen-Chowdhry, S., and McKenna, W.J. *'Arrhythmogenic right ventricular dysplasia/cardiomyopathy associated with mutations in the desmosomal gene desmocollin-2'.* 2006., Am. J. Hum. Genet., 79: 978-984

Thiene, G., Corrado, D., Nava, A., Rossi, L., Poletti, A., Boffa, G.M., Daliento, L., and Pennelli, N. *'Right ventricular cardiomyopathy: is there evidence of an inflammatory aetiology?'.* 1991., Eur. Heart J., 12 Suppl D: 22-25

Thiene, G., Nava, A., Corrado, D., Rossi, L., and Pennelli, N. *'Right ventricular cardiomyopathy and sudden death in young people'.* 1988., N. Engl. J. Med., 318: 129-133

Thiene, G. *'The research venture in arrhythmogenic right ventricular cardiomyopathy: a paradigm of translational medicine'.* 2015., Eur. Heart J., 36: 837-846

Thiene, G., Corrado, D., and Basso, C. *'Arrhythmogenic right ventricular cardiomyopathy/dysplasia'.* 2007., Orphanet J Rare Dis, 2: 45

Thum, T., Gross, C., Fiedler, J., Fischer, T., Kissler, S., Bussen, M., Galuppo, P., Just, S., Rottbauer, W., Frantz, S., Castoldi, M., Soutschek, J., Koteliansky, V., Rosenwald, A., Basson, M.A., Licht, J.D., Pena, J.T.R., Rouhanifard, S.H., Muckenthaler, M.U., Tuschl, T., Martin, G.R., Bauersachs, J., and Engelhardt, S. *'MicroRNA-21 contributes to myocardial disease by stimulating MAP kinase signalling in fibroblasts'.* 2008., Nature, 456: 980-984

Tony, H., Meng, K., Wu, B., Yu, A., Zeng, Q., Yu, K., and Zhong, Y. *'MicroRNA-208a Dysregulates Apoptosis Genes Expression and Promotes Cardiomyocyte Apoptosis during Ischemia and Its Silencing Improves Cardiac Function after Myocardial Infarction'.* 2015., Mediators Inflamm., 2015: 479123

van Rooij, E., Quiat, D., Johnson, B.A., Sutherland, L.B., Qi, X., Richardson, J.A., Kelm, R.J., and Olson, E.N. *'A family of microRNAs encoded by myosin genes governs myosin expression and muscle performance'.* 2009., Dev. Cell, 17: 662-673

van Rooij, E., Sutherland, L.B., Liu, N., Williams, A.H., McAnally, J., Gerard, R.D., Richardson, J.A., and Olson, E.N. *'A signature pattern of stress-responsive microRNAs that can evoke cardiac hypertrophy and heart failure'.* 2006., Proc. Natl. Acad. Sci. U.S.A., 103: 18255-18260

Wang, H., Chen, F., Tong, J., Li, Y., Cai, J., Wang, Y., Li, P., Hao, Y., Tian, W., Lv, Y., Chong, J., and Yang, J. *'Circulating microRNAs as novel biomarkers for dilated cardiomyopathy'.* 2017., Cardiology Journal, 24: 65-73

Wang, J., Pei, Y., Zhong, Y., Jiang, S., Shao, J., and Gong, J. *'Altered serum microRNAs as novel diagnostic biomarkers for atypical coronary artery disease'.* 2014., PLoS ONE, 9: e107012

Wang, X., Zhang, X., Ren, X., Chen, J., Liu, H., Yang, J., Medvedovic, M., Hu, Z., and Fan, G. *'MicroRNA-494 targeting both proapoptotic and antiapoptotic proteins protects against ischemia/reperfusion-induced cardiac injury'.* 2010., Circulation, 122: 1308-1318

Webber, J., Steadman, R., Mason, M.D., Tabi, Z., and Clayton, A. *'Cancer exosomes trigger fibroblast to myofibroblast differentiation'.* 2010., Cancer Res., 70: 9621-9630

Wei, Y., Yan, X., Yan, L., Hu, F., Ma, W., Wang, Y., Lu, S., Zeng, Q., and Wang, Z. *'Inhibition of microRNA-155 ameliorates cardiac fibrosis in the process of angiotensin II-induced cardiac remodeling'.* 2017., Mol Med Rep

Wijnen, W.J., van der Made, I., van den Oever, S., Hiller, M., de Boer, B.A., Picavet, D.I., Chatzispyrou, I.A., Houtkooper, R.H., Tijsen, A.J., Hagoort, J., van Veen, H., Everts, V., Ruijter, J.M., Pinto, Y.M., and Creemers, E.E. *'Cardiomyocyte-specific*

miRNA-30c over-expression causes dilated cardiomyopathy'. 2014., PLoS ONE, 9: e96290

Winter, J., Jung, S., Keller, S., Gregory, R.I., and Diederichs, S. *'Many roads to maturity: microRNA biogenesis pathways and their regulation'.* 2009., Nat. Cell Biol., 11: 228-234

Yamada, S., Hsiao, Y., Chang, S., Lin, Y., Lo, L., Chung, F., Chiang, S., Hu, Y., Tuan, T., Chao, T., Liao, J., Lin, C., Chang, Y., Te, A.L.D., Tsai, Y., and Chen, S. *'Circulating microRNAs in arrhythmogenic right ventricular cardiomyopathy with ventricular arrhythmia'.* 2017., Europace

Yao, X., Lu, X., Yan, C., Wan, Q., Cheng, G., and Li, Y. *'Circulating miR-122-5p as a potential novel biomarker for diagnosis of acute myocardial infarction'.* 2015., Int J Clin Exp Pathol, 8: 16014-16019

Yi, R., Qin, Y., Macara, I.G., and Cullen, B.R. *'Exportin-5 mediates the nuclear export of pre-microRNAs and short hairpin RNAs'.* 2003., Genes Dev., 17: 3011-3016

Yu, D., Li, Q., Ding, X., and Ding, Y. *'Circulating microRNAs: potential biomarkers for cancer'.* 2011., Int J Mol Sci, 12: 2055-2063

Yuan, X., Liu, C., Yang, P., He, S., Liao, Q., Kang, S., and Zhao, Y. *'Clustered microRNAs' coordination in regulating protein-protein interaction network'.* 2009., BMC Syst Biol, 3: 65

Zhang, H., Liu, S., Dong, T., Yang, J., Xie, Y., Wu, Y., Kang, K., Hu, S., Gou, D., and Wei, Y. *'Profiling of differentially expressed microRNAs in arrhythmogenic right ventricular cardiomyopathy'.* 2016., Scientific reports, 6: 28101

Zhang, X., Wang, X., Zhu, H., Zhu, C., Wang, Y., Pu, W.T., Jegga, A.G., and Fan, G. *'Synergistic effects of the GATA-4-mediated miR-144/451 cluster in protection against simulated ischemia/reperfusion-induced cardiomyocyte death'.* 2010., J. Mol. Cell. Cardiol., 49: 841-850

Zhou, Q., Schötterl, S., Backes, D., Brunner, E., Hahn, J.K., Ionesi, E., Aidery, P., Sticht, C., Labeit, S., Kandolf, R., Gawaz, M., and Gramlich, M. *'Inhibition of miR-208b improves cardiac function in titin-based dilated cardiomyopathy'.* 2017., Int. J. Cardiol., 230: 634-641

Zweig, M.H., and Campbell, G. *'Receiver-operating characteristic (ROC) plots: a fundamental evaluation tool in clinical medicine'.* 1993., Clin. Chem., 39: 561-577

7 Appendix A: Abbreviations

AC: Arrhythmogenic Cardiomyopathy.

AS: Aortic Stenosis.

AUC: Area Under the ROC curve.

AMI: Acute Myocardial Infarction.

CAD: Coronary Artery Disease.

cDNA: complementary DNA.

DCM: Dilated Cardiomyopathy.

dsDNA: double-stranded DNA.

dsRNA: double-stranded RNA.

ECM: Extracellular Matrix.

HC: Healthy Controls.

HCM: Hypertrophic Cardiomyopathy.

HF: Heart Failure.

HCNM: Hypertrophic Non-Obstructive Cardiomyopathy.

HOCM: Hypertrophic Obstructive Cardiomyopathy.

ID: Intercalated Disc.

IVT: Idiopathic Ventricular Tachycardia.

LBBB: Left Bundle Branch Block.

LV: Left Ventricle.

MPC: Mesenchymal Progenitor Cell.

miRNA: microRNA.

miRNP: microRNA ribonucleoprotein complex.

PBMC: Peripheral Mononuclear Cell.

qPCR: Real-Time PCR.

RNAi: RNA interference.

RISC: RNA-interference silencing complex.

ROC: Receiver Operating Characteristic.

RV: Right Ventricle.

siRNA: small interference RNA.

SNORD68: Small Nucleolar RNA, C/D box 68.

stRNA: small temporal RNA.

Tm: Melting Temperature.

VA: Ventricular Arrhythmia.